MOLECULAR PHYSICS, 1996, VOL. 89, NO. 1, 81–110

Symmetry-adapted perturbation theory applied to interaction-induced properties of collisional complexes

By TINO G. A. HEIJMEN†, ROBERT MOSZYNSKI†‡,
PAUL E. S. WORMER† and AD VAN DER AVOIRD†

† Institute of Theoretical Chemistry, NSR Center, Toernooiveld 1, University of Nijmegen, 6525 ED Nijmegen, The Netherlands

‡ Department of Chemistry, University of Warsaw, Pasteura 1, 02-093 Warsaw, Poland

(*Received 9 December 1995; accepted 14 February 1996*)

A symmetry-adapted perturbation theory (SAPT) is formulated for interaction-induced electrical properties of weakly bound complexes. Asymptotic (large R) expressions are reported for the contributions to the collision-induced dipole moments and polarizabilities up to and including second order in the intermolecular potential. These long-range expressions require knowledge only of the multipole moments and (hyper)polarizabilities of the isolated monomers. Numerical results are given for the dipole moment of $He–H_2$ and the polarizability of He_2 and the accuracy of the SAPT approach is examined by comparison with full configuration interaction results. The role of various physical contributions to the dipole moment of $He–H_2$ and the polarizability of He_2 is investigated. The validity of the long-range approximation and the importance of charge penetration (damping) effects are discussed.

1. Introduction

During a collision between two molecules the intermolecular interaction leads to distortions of their charge distributions, so that a collisional complex may possess a dipole moment and polarizability in excess of the sum of these properties of the isolated molecules. These excess properties, referred to as the interaction-induced or collision-induced dipole moment and polarizability are defined as incremental parts of the properties of the complex A–B due to intermolecular interactions.

The interaction-induced dipole moments and polarizabilities are responsible for a wide range of dielectric, refractive, and optical properties of gases and fluids [1, 2]. In pioneering studies Crawford *et al.* [3] and Chisholm and Welsh [4] have shown that during a collision of a helium atom with a hydrogen molecule the complex becomes temporarily infrared-active because of its relative translational motions, so that absorption and emission bands can be observed. Much work has been done on the measurements of these collision-induced spectra; see, for instance, a recent monograph by Frommhold [5] for an interview review.

Levine and Birnbaum [6] predicted that all Raman spectra of gases should have a component caused by collision-induced changes in the polarizabilities. Indeed, it was demonstrated first by McTague and Birnbaum [7, 8] that colliding argon atoms undergo transitions between translational states when interacting with photons. These transitions are due exclusively to the collision-induced light scattering, i.e., to interaction-induced fluctuations of the polarizabilities of the atoms and molecules.

0026–8976/96 $12·00

Since the early work on argon, collision-induced light scattering has been studied experimentally in several optically isotropic systems (see [9] for a review).

Despite the growing body of experimental work on collision-induced absorption and light scattering, not many numerical studies have been devoted to the mechanisms that yield the collision-induced properties themselves. Most *ab initio* calculations were limited to the Hartree–Fock level (see, e.g. [10] and [11]). In a series of papers Meyer and Frommhold [12–18] have shown that dipole moment contributions from intramonomer and intermonomer electronic correlation are both substantial. At present, supermolecular results from correlated *ab initio* calculations are available for a limited numbers of systems: dipole moments of He–H [12], He–Ar [13], He–F^- and He–Cl^- [19], He–H_2 [14, 15, 20], Ar–H_2 [16], H_2–H_2 [17, 18], and polarizabilities of He_2 [21–23], Ne_2 [24], He–F^- and He–Cl^- [19], and He–CH_4 [25] (see also [26] and [27] for recent reviews), and only a few of these dipole and polarizability surfaces have been applied to generate collision-induced infrared [12, 13, 15–18, 28] and Raman spectra [23, 29].

On the other hand, perturbation theory studies of the interaction–induced properties have been based mainly on the Rayleigh–Schrödinger polarization treatment (with neglect of the electron exchange) coupled with the multipole expansion of the intermolecular interaction operator (with neglect, in turn, of charge overlap (damping) effects) [30–42] (see also [43–47] for papers describing computations of the long-range coefficients for the interaction induced dipole moments and polarizabilities of various dimers). Moreover, the asymptotic expressions derived in the framework of the multipole approximation pertain to specific systems, and are usually restricted to the leading power of the reciprocal intermolecular distance. Applications of various exchange perturbation theory schemes to interaction-induced properties are scarce, and limited to the simplest approximations [48–55]. Consequently, very little is known about the importance of the charge overlap and exchange effects.

Recently, the many-body formulation [56–63] of the symmetry-adapted perturbation theory (SAPT) of intermolecular interactions [64–67] has been developed. In this approach all physically important contributions to the potential, such as electrostatics, exchange, induction, and dispersion, are identified and computed separately. By making a perturbation expansion in the intermolecular interaction as well as in the intramolecular electronic correlation, it is possible to sum the correlation contributions to the different physical effects only as far as necessary. The SAPT approach does not use the multipole expansion [68, 69], so all charge penetration (damping) effects are included automatically. Since various contributions to the interaction energy show a different dependence on the intermolecular distance R, they can be fitted separately, with adjustable and physically interpretable parameters [71, 72]. This method has been applied to determine interaction potentials for the He–K^+ [73], He–Na^+ [74], Ar–H_2 [75], He–HF [76], He–C_2H_2 [77], He–CO [78], and Ar–HF [79] systems (see [80] for a recent review of SAPT theory and applications). In most cases, excellent agreement is achieved when compared with the accurately determined (semi)empirical potentials available for these systems. The SAPT potentials have been used to generate the far- and near-infrared spectra of Ar–H_2 [81], and the near-infrared spectra of He–HF [82], He–C_2H_2 [77], and He–CO [78]. In general, the resulting line positions are in very good agreement with the experimental data (see [83] for a review of dynamical calculations).

Since the SAPT theory of intermolecular interactions is well developed, it is natural to study its applicability to interaction-induced properties. It is the aim of this paper

to report such a study. The plan of this paper is as follows. In section 2 we formulate the symmetry-adapted perturbation theory approach to interaction-induced properties. In section 3 we present open-ended multipole-expanded formulas for the polarization contributions to the interaction-induced dipole moments and dipole polarizabilities through the second-order of perturbation theory. In section 4 we describe computational details. In section 5 we apply the theory of sections 2 and 3 to the interaction-induced dipole moment of $He–H_2$ and the polarizability of He_2. By comparison with full configuration interaction (FCI) results we study the applicability of the many-body SAPT expansion to interaction-induced dipole moments and polarizabilities of model systems. We discuss the role of various physical contributions to the interaction-induced dipole moment and polarizability, investigate the validity of the multipole expansion, and study the importance of the charge overlap (damping) effects. Finally, in section 6 we present conclusions.

2. Symmetry-adapted perturbation theory of the interaction-induced properties

The interaction-induced dipole moment of a pair of molecules A and B is given by the difference between the dipole moment of the complex A–B and the sum of dipole moments of the non-interacting molecules A and B,

$$\Delta\mu_i = \mu_i^{AB} - \mu_i^{A} - \mu_i^{B}, \tag{1}$$

where μ_i^{AB} is a Cartesian component of the dipole moment of the dimer A–B, and μ_i^{A} and μ_i^{B} denote components of the dipole moments of the isolated molecules A and B, respectively. Similarly, the interaction-induced polarizability of a pair of molecules A and B is defined as the excess polarizability of the collisional pair A–B due to intermolecular interactions, i.e.,

$$\Delta\alpha_{ij} = \alpha_{ij}^{AB} - \alpha_{ij}^{A} - \alpha_{ij}^{B}, \tag{2}$$

where α_{ij}^{AB} is a Cartesian component of the dimer polarizability tensor, and α_{ij}^{A} and α_{ij}^{B} denote components of the polarizability tensors of the isolated monomers A and B, respectively. Equations (1) and (2) can be rewritten conveniently as

$$\Delta\mu_i = -\left(\frac{\partial E_{\text{int}}}{\partial F_i}\right)_{\mathbf{F}=\mathbf{0}}, \tag{3}$$

$$\Delta\alpha_{ij} = -\left(\frac{\partial^2 E_{\text{int}}}{\partial F_i \partial F_j}\right)_{\mathbf{F}=\mathbf{0}}, \tag{4}$$

where E_{int} is the interaction energy for the dimer A–B in the presence of a static, uniform electric field **F**. Equations (3) and (4) show that the interaction-induced dipole moment and polarizability can be obtained from standard finite field calculations, if the field-dependent interaction energy can be computed. In the present paper we have utilized this possibility, i.e., first we performed calculations of the interaction energy in the static electric field using the symmetry-adapted perturbation theory, and subsequently we obtained the interaction-induced dipole moments and polarizabilities from finite difference formulas.

The SAPT approach calculates the interaction energy E_{int} directly, as a sum of physically distinct polarization and exchange contributions,

$$E_{\text{int}} = E_{\text{pol}}^{(1)} + E_{\text{exch}}^{(1)} + E_{\text{pol}}^{(2)} + E_{\text{exch}}^{(2)} + \dots, \tag{5}$$

where $E_{\text{pol}}^{(1)}$ is the classical electrostatic energy calculated with full account of the charge-overlap (penetration) effects, and $E_{\text{pol}}^{(2)}$ is the sum of the induction and dispersion energies, $E_{\text{pol}}^{(2)} = E_{\text{ind}}^{(2)} + E_{\text{disp}}^{(2)}$, rigorously damped by the charge-overlap effects. $E_{\text{exch}}^{(1)}$ and $E_{\text{exch}}^{(2)}$ are the exchange contributions in the first and second order in the intermolecular potential, respectively. They can be interpreted physically as an effect of the resonance tunnelling of electrons between the interacting systems. In the second order it is possible to split the exchange term into an induction part and a dispersion part, $E_{\text{exch}}^{(2)} = E_{\text{exch-ind}}^{(2)} + E_{\text{exch-disp}}^{(2)}$. The exchange–induction energy $E_{\text{exch-ind}}^{(2)}$ and the exchange–dispersion energy $E_{\text{exch-disp}}^{(2)}$ represent the effect of the antisymmetrization of the first-order induction and dispersion wavefunctions, and can be viewed as a result of the coupling of the electron exchange with the induction and dispersion interaction. In view of equations (3) and (4), the components of the interaction-induced dipole moment and polarizability can be written as,

$$\Delta\mu_i = \Delta\mu_{i,\text{pol}}^{(1)} + \Delta\mu_{i,\text{exch}}^{(1)} + \Delta\mu_{i,\text{pol}}^{(2)} + \Delta\mu_{i,\text{exch}}^{(2)} + \dots, \tag{6}$$

$$\Delta\alpha_{ij} = \Delta\alpha_{ij,\text{pol}}^{(1)} + \Delta\alpha_{ij,\text{exch}}^{(1)} + \Delta\alpha_{ij,\text{pol}}^{(2)} + \Delta\alpha_{ij,\text{exch}}^{(2)} + \dots, \tag{7}$$

where the superscripts again indicate the order in the intermolecular potential. Obviously an nth order contribution to $\Delta\mu_i$ or $\Delta\alpha_{ij}$ is obtained by differentiating once or twice the corresponding contribution of the nth order interaction energy, cf. equation (3)–(5).

Equation (6) relates the interaction-induced part of the dipole moment of the complex A–B to the distortion of the electron density associated with the electrostatic, exchange, induction, and dispersion interaction energies of the monomers in the external electrostatic field. The polarization contributions to the dipole moment through the second order of perturbation theory ($\Delta\mu_{i,\text{pol}}^{(1)}$, $\Delta\mu_{i,\text{ind}}^{(2)}$, and $\Delta\mu_{i,\text{disp}}^{(2)}$) have an appealing, partly classical, partly quantum, physical interpretation, and can be obtained also from the multipole approximation. Basically there are two points of view: the finite field approach considers the terms of the interaction energies which are linear in an external field, whereas the perturbation approach considers expectation values of the dimer dipole operator. From the finite field point of view the first-order multipole-expanded polarization contribution $E_{\text{pol}}^{(1)}$ is due to the interactions of permanent multipole moments on A with moments induced on B by the external field **F**, and vice versa. The terms linear in **F** give $\Delta\mu_{i,\text{pol}}^{(2)}$. The mechanism that yields the second-order induction dipole $\Delta\mu_{i,\text{ind}}^{(1)}$ is somewhat more complicated, and one can distinguish two principal categories. The first mechanism is the interaction of a permanent multipole on monomer A with a multipole on B induced by the nonlinear (second-order) effect of both a permanent multipole on A and the external field **F** (plus a contribution obtained by interchanging the roles of the monomers A and B). The second mechanism is the interaction of a multipole moment on A, induced by a permanent multipole on B, with a moment on B induced by the external field **F**, and vice versa. Again, the energy terms that are linear in **F** give the corresponding interaction induced dipoles. In section 3.1 we will return to the perturbation interpretation of these quantities. Finally, the dispersion term $\Delta\mu_{i,\text{disp}}^{(2)}$ represents the

intermonomer correlation contribution to the dipole moment of the dimer A–B. The various physical contributions to the interaction-induced polarizability can be classified analogously.

For interactions of many-electron systems one has to use the many-body version of SAPT, which includes order by order the intramonomer correlation effects. The many-body SAPT is based on the partitioning of the total Hamiltonian as $H = F + V + W$, where the zero-order operator $F = F_A + F_B$ is the sum of the Fock operators for the monomers A and B. The intermolecular interaction operator $V = H - H_A - H_B$ is the difference between the Hamiltonians of interacting and noninteracting systems, and the intramonomer correlation operator $W = W_A + W_B$ is the sum of the Møller–Plesset fluctuation potentials of the monomers: $W_X = H_X - F_X$, X = A or B. The interaction operator V is taken in the non-expanded form, i.e., it is not approximated by the multipole expansion. The interaction energy components of equation (5) are now given in the form of a double perturbation series

$$E_{pol}^{(n)} = \sum_{l=0}^{\infty} E_{pol}^{(nl)} \quad \text{and} \quad E_{exch}^{(n)} = \sum_{l=0}^{\infty} E_{exch}^{(nl)}, \tag{8}$$

where the superscripts n and l at $E_{pol}^{(nl)}$ and $E_{exch}^{(nl)}$ denote the orders of perturbation in V and in W, respectively. Note that also the induction and dispersion parts of $E_{pol}^{(2)}$ and $E_{exch}^{(2)}$ can be written as $E_{pol}^{(2l)} = E_{ind}^{(2l)} + E_{disp}^{(2l)}$ and $E_{exch}^{(2l)} = E_{exch-ind}^{(2l)} + E_{exch-disp}^{(2l)}$. For further discussion it is useful to introduce the quantities

$$\varepsilon_{pol}^{(n)} \equiv \sum_{l=1}^{\infty} E_{pol}^{(nl)} \quad \text{and} \quad \varepsilon_{exch}^{(n)} \equiv \sum_{l=1}^{\infty} E_{exch}^{(nl)}, \tag{9}$$

which represent the cumulative effect of all intramonomer correlation contributions to $E_{pol}^{(n)}$ and $E_{exch}^{(n)}$, respectively.

It can be shown [84–87] that the Hartree–Fock interaction energy E_{int}^{HF}, defined as the difference between the Hartree–Fock energies for the complex and for the free monomers, is a sum of certain SAPT contributions under neglect of the intermonomer and intramonomer correlation effects. Specially, the terms $E_{pol}^{(10)}$, $E_{exch}^{(10)}$, $E_{ind}^{(20)}$, $E_{exch-ind}^{(20)}$, and some higher-order induction and exchange contributions are included in E_{int}^{HF}. Thus, E_{int}^{HF} can be represented as

$$E_{int}^{HF} = E_{pol}^{(10)} + E_{exch}^{(10)} + E_{ind,resp}^{(20)} + E_{exch-ind,resp}^{(20)} + \delta E_{int}^{HF}, \tag{10}$$

where $E_{ind,resp}^{(20)}$ and $E_{exch-ind,resp}^{(20)}$ are the second-order induction [62, 86] and exchange-induction energies [87] calculated with the inclusion of the coupled Hartree–Fock type response of a perturbed system and δE_{int}^{HF} collects all higher-order induction and exchange terms.

Equation (10) allows one to incorporate the Hartree–Fock interaction energy E_{int}^{HF} into the expression for E_{int} by replacing in equation (5) the low-order energy contributions, given explicitly in equation (10), by the Hartree–Fock interaction energy E_{int}^{HF}. We used this possibility, and the field-dependent interaction energy computed in this work is defined as

$$E_{int} = E_{int}^{HF} + \varepsilon_{pol}^{(1)} + \varepsilon_{exch}^{(1)} + \varepsilon_{ind}^{(2)} + E_{disp}^{(2)} + E_{exch-disp}^{(2)}. \tag{11}$$

In practice, one has to truncate the expansions (8) and (9). Recent studies of the convergence of the many-body perturbation expansions of the electrostatic [59],

exchange [60, 62], induction [62], and dispersion [63] energies for weakly bound complexes have shown that the following approximations are sufficient to reproduce the interaction energy with an error of a few per cent or less:

$$\varepsilon_{\mathrm{pol}}^{(1)} = E_{\mathrm{pol,resp}}^{(12)} + E_{\mathrm{pol,resp}}^{(13)}, \tag{12}$$

$$\varepsilon_{\mathrm{exch}}^{(1)} = E_{\mathrm{exch}}^{(11)} + E_{\mathrm{exch}}^{(12)} + \Delta_{\mathrm{exch}}^{(1)}(\mathrm{CCSD}), \tag{13}$$

$$\varepsilon_{\mathrm{ind}}^{(2)} = \varepsilon_{\mathrm{ind}}^{(22)}, \tag{14}$$

$$E_{\mathrm{disp}}^{(2)} = E_{\mathrm{disp}}^{(20)} + E_{\mathrm{disp}}^{(21)} + E_{\mathrm{disp}}^{(22)}, \tag{15}$$

$$E_{\mathrm{exch-disp}}^{(2)} = E_{\mathrm{exch-disp}}^{(20)}. \tag{16}$$

The electrostatic corrections $E_{\mathrm{pol,resp}}^{(1n)}$ are defined as in [59]. The first-order exchange components $E_{\mathrm{exch}}^{(1n)}$ are defined as in [60] and [61], while $\Delta_{\mathrm{exch}}^{(1)}$ (CCSD) is the sum of higher-order terms (in the intramonomer correlation) obtained by replacing the first- and second-order cluster operators entering the expression for $E_{\mathrm{exch}}^{(12)}$ by the converged coupled-cluster singles and doubles (CCSD) operators [60]. The induction term $\varepsilon_{\mathrm{ind}}^{(22)}$ represents the true correlation contribution to the non-relaxed correction $E_{\mathrm{ind}}^{(22)}$, as defined in [62]. The dispersion components $E_{\mathrm{disp}}^{(2n)}$ are derived in [58]. Finally, $E_{\mathrm{exch-disp}}^{(20)}$ is the so-called Hartree–Fock exchange–dispersion energy [89].

3. The multipole expansion of the interaction-induced electric properties

In this section we will give the asymptotic (large R) expressions for the electrostatic, induction, and dispersion contributions to the interaction-induced dipole moment and polarizability by introducing the multipole expansion of the intermolecular interaction operator through second-order perturbation theory. The great advantage of the multipole expansion is that it yields expressions for the interaction-induced properties in which properties only of the free monomers appear. An additional advantage is that the geometry dependence is given explicitly in terms of simple functions. We shall use the spherical form of the multipole expansion since, in contrast to the Cartesian formalism, it gives the orientational dependence of the interaction energy components in closed form. Because the spherical expressions found in the literature [36, 42] pertain to specific systems and are usually restricted to the leading powers of the $1/R$ expansion, we report below open-ended asymptotic formulas for the first- and second-order contributions to the interaction-induced dipole moment and polarizability. In particular, we show how the electrostatic, induction, and dispersion contributions to these properties can be written solely in terms of the following monomer properties: multipole moments, polarizabilities and hyperpolarizabilities.

In the derivations of the expressions in this section the monomer properties are initially expressed with respect to an arbitrary space-fixed frame. Since the electric properties are usually calculated or measured with respect to axes fixed to the molecule, we then transform from the space-fixed to the body-fixed frame of either monomer. The angular momentum coupling used in all our formulas has the purpose of making this transformation as simple as possible. All properties on each monomer are coupled to spherical tensors of rank L_{X}, X = A, B, which transform under the frame rotation by the use of irreducible Wigner rotation matrices $\mathbf{D}^{L\mathrm{X}}(\boldsymbol{\omega}_{\mathrm{X}})$ [90]. Here $\boldsymbol{\omega}_{\mathrm{X}}$ is a set of three Euler angles of monomer X. These angles describe the rotation of a frame parallel to the space-fixed frame (with its origin in the mass centre of X), so

that it coincides with the body-fixed frame X. The geometry dependence of various physical contributions to the interaction induced dipole moment and polarizability is thus described by a product of two D matrices, one for each monomer, times a function depending on the spherical polar coordinates of the vector **R** pointing from the nuclear centre of mass of monomer A to that of monomer B, cf. equation (23) below. We designate the polar angles of **R** with respect to a space-fixed frame by $\hat{\mathbf{R}}$ (which is a unit vector along **R**), and its length by R.

The quantity Q^l_m denotes the monomer expectation value of a component of the multipole operator with rank l,

$$Q^l_m \equiv \langle 0|\hat{Q}^l_m|0\rangle, \tag{17}$$

where

$$\hat{Q}^l_m \equiv \sum_{i=1}^{N} Z_i r_i^l C^l_m(\theta_i, \phi_i) \tag{18}$$

is a sum over the particles of the monomer with charge Z_i and polar coordinates r_i, θ_i, ϕ_i. The function C^l_m is a spherical harmonic function normalized to $4\pi/(2l+1)$. Below we consider multipoles belonging to monomer A or B, which will be indicated by a corresponding subscript on the indices. We will designate a reducible frequency-dependent polarizability by

$$\alpha^{ll'}_{mm'}(\omega) \equiv 2 \sum_{n\neq 0} \frac{E_n - E_0}{(E_n - E_0)^2 - \omega^2} \langle 0|\hat{Q}^l_m|n\rangle \langle n|\hat{Q}^{l'}_{m'}|0\rangle, \tag{19}$$

where $|n\rangle$, $n = 0, 1, \ldots$ are the molecular eigenstates with eigenvalues E_n. The corresponding irreducible polarizability $\alpha^{(ll')\lambda}_{\mu}(\omega)$ is obtained by Clebsch–Gordan coupling,

$$\alpha^{(ll')\lambda}_{\mu}(\omega) \equiv \sum_{m,m'} \langle l, m; l', m' \,|\, \lambda, \mu\rangle \, \alpha^{ll'}_{mm'}(\omega). \tag{20}$$

Often the Clebsch–Gordan coupled product of spherical tensors will also be denoted as $[\mathbf{T}^l \otimes \mathbf{S}^{l'}]^{\mathrm{L}}$, i.e., as a binary product between square brackets,

$$[\mathbf{T}^l \otimes \mathbf{S}^{l'}]^L_M = \sum_{m,m'} \langle l, m; l', m' \,|\, L, M\rangle \, T^l_m \, S^{l'}_{m'}. \tag{21}$$

The multipole-expanded expressions for the electrostatic, induction, and dispersion contributions to the interaction-induced dipole moments and dipole–dipole polarizabilities can be obtained by applying double perturbation theory to the Schrödinger equation with the Hamiltonian

$$H = H_0 + \tilde{V} + \sum_m (-1)^m F_{-m} \hat{Q}^1_m, \tag{22}$$

where H_0 is the sum of Hamiltonians of the isolated monomers, $\tilde{V}$ is the intermolecular interaction operator, with the tilde indicating that it is in the multipole approximation, $\hat{Q}^1_m$ is the spherical component of the sum of the dipole operators on A and B, and F_{-m}

denotes a component of an external homogeneous static electric field. Alternatively, the multipole-expanded formulas can be found by applying equations (3) and (4) to the multipole-expanded expressions for $E^{(1)}_{\mathrm{pol}}$, $E^{(2)}_{\mathrm{ind}}$, and $E^{(2)}_{\mathrm{disp}}$. Since the final expressions for the interaction-induced properties in the multipole approximation are quite involved, we have followed both routes of derivation to check the correctness of our formulas. The required multipole-expanded expressions for the second-order interaction energies are given in [69].

Introducing $\{\Lambda\} = \{L_{\mathrm{A}}, K_{\mathrm{A}}, L_{\mathrm{B}}, K_{\mathrm{B}}, L\}$ we define an irreducible tensorial set of angular expansion functions

$$A^{(\lambda)l}_{\{\Lambda\}m}(\boldsymbol{\omega}_{\mathrm{A}}, \boldsymbol{\omega}_{\mathrm{B}}, \hat{\mathbf{R}}) = \sum_{M_{\mathrm{A}}=-L_{\mathrm{A}}}^{L_{\mathrm{A}}} \sum_{M_{\mathrm{B}}=-L_{\mathrm{B}}}^{L_{\mathrm{B}}} \sum_{\mu=-\lambda}^{\lambda} \sum_{M=-L}^{L} \langle L_{\mathrm{A}}, M_{\mathrm{A}}; L_{\mathrm{B}}, M_{\mathrm{B}} | \lambda, \mu\rangle \langle \lambda, \mu; L, M | l, m\rangle$$
$$\times D^{L_{\mathrm{A}}}_{M_{\mathrm{A}},K_{\mathrm{A}}}(\boldsymbol{\omega}_{\mathrm{A}})^{*}\, D^{L_{\mathrm{B}}}_{M_{\mathrm{B}},K_{\mathrm{B}}}(\boldsymbol{\omega}_{\mathrm{B}})^{*} C^{L}_{M}(\hat{\mathbf{R}}). \tag{23}$$

When we expand a scalar property with $l = m = 0$, such as the energy, this expression can be simplified by noting that the product of two Clebsch–Gordan coefficients in the angular function $A^{(L)0}_{\{\Lambda\}0}(\boldsymbol{\omega}_{\mathrm{A}}, \boldsymbol{\omega}_{\mathrm{B}}, \hat{\mathbf{R}})$ reduces to a $3jm$ symbol [90],

$$\sum_{\mu=-L}^{L} \langle L_{\mathrm{A}}, M_{\mathrm{A}}; L_{\mathrm{B}}, M_{\mathrm{B}} | L, \mu\rangle \langle L, \mu; L, M | 0, 0\rangle = (-1)^{L_{\mathrm{A}}+L_{\mathrm{B}}+L} \begin{pmatrix} L_{\mathrm{A}} & L_{\mathrm{B}} & L \\ M_{\mathrm{A}} & M_{\mathrm{B}} & M \end{pmatrix}. \tag{24}$$

We will, however, work with Clebsch–Gordan coupled angular functions throughout this paper, and also when expanding interaction energies. The energy coefficients of the angular functions in equation (23) for $E^{(1)}_{\mathrm{pol}}$, $E^{(2)}_{\mathrm{ind}}$, and $E^{(2)}_{\mathrm{disp}}$ are

$$\Delta E^{(1)}_{\mathrm{mult},\{\Lambda\}} = (-1)^{L_{\mathrm{A}}} \delta_{L_{\mathrm{A}}+L_{\mathrm{B}},L}\, R^{-(L_{\mathrm{A}}+L_{\mathrm{B}}+1)} \left[\frac{(2L_{\mathrm{A}}+2L_{\mathrm{B}}+1)!}{(2L_{\mathrm{A}})!(2L_{\mathrm{B}})!}\right]^{1/2} Q^{L_{\mathrm{A}}}_{K_{\mathrm{A}}}\, Q^{L_{\mathrm{B}}}_{K_{\mathrm{B}}}, \tag{25}$$

$$\Delta E^{(2)}_{\mathrm{ind,mult},\{\Lambda\}} = -\frac{1}{2} \sum_{l_{\mathrm{A}},l'_{\mathrm{A}},l_{\mathrm{B}},l'_{\mathrm{B}}} R^{-(l_{\mathrm{A}}+l'_{\mathrm{A}}+l_{\mathrm{B}}+l'_{\mathrm{B}}+2)}\, \zeta^{L_{\mathrm{A}}L_{\mathrm{B}}L}_{l_{\mathrm{A}}l'_{\mathrm{A}}l_{\mathrm{B}}l'_{\mathrm{B}}} \begin{Bmatrix} l_{\mathrm{A}} & l'_{\mathrm{A}} & L_{\mathrm{A}} \\ l_{\mathrm{B}} & l'_{\mathrm{B}} & L_{\mathrm{B}} \\ l_{\mathrm{A}}+l_{\mathrm{B}} & l'_{\mathrm{A}}+l'_{\mathrm{B}} & L \end{Bmatrix}$$
$$\times (1+\hat{\mathscr{P}}_{\mathrm{AB}})\, \alpha^{(l_{\mathrm{A}}l'_{\mathrm{A}})L_{\mathrm{A}}}_{K_{\mathrm{A}}}(0)\, [\mathbf{Q}^{l_{\mathrm{B}}} \otimes \mathbf{Q}^{l'_{\mathrm{B}}}]^{L_{\mathrm{B}}}_{K_{\mathrm{B}}}, \tag{26}$$

$$\Delta E^{(2)}_{\mathrm{disp,mult},\{\Lambda\}} = -\sum_{l_{\mathrm{A}},l'_{\mathrm{A}},l_{\mathrm{B}},l'_{\mathrm{B}}} R^{-(l_{\mathrm{A}}+l'_{\mathrm{A}}+l_{\mathrm{B}}+l'_{\mathrm{B}}+2)}\, \zeta^{L_{\mathrm{A}}L_{\mathrm{B}}L}_{l_{\mathrm{A}}l'_{\mathrm{A}}l_{\mathrm{B}}l'_{\mathrm{B}}} \begin{Bmatrix} l_{\mathrm{A}} & l'_{\mathrm{A}} & L_{\mathrm{A}} \\ l_{\mathrm{B}} & l'_{\mathrm{B}} & L_{\mathrm{B}} \\ l_{\mathrm{A}}+l_{\mathrm{B}} & l'_{\mathrm{A}}+l'_{\mathrm{B}} & L \end{Bmatrix}$$
$$\times \frac{1}{2\pi} \int_0^{\infty} \alpha^{(l_{\mathrm{A}}l'_{\mathrm{A}})L_{\mathrm{A}}}_{K_{\mathrm{A}}}(i\omega)\, \alpha^{(l_{\mathrm{B}}l'_{\mathrm{B}})L_{\mathrm{B}}}_{K_{\mathrm{B}}}(i\omega)\, \mathrm{d}\omega, \tag{27}$$

respectively, where $\hat{\mathscr{P}}_{\mathrm{AB}}$ interchanges all symbols pertaining to molecules A and B, while the quantity between large curly braces is a $9j$ symbol [90]. The algebraic coefficient $\zeta^{L_{\mathrm{A}}L_{\mathrm{B}}L}_{l_{\mathrm{A}}l'_{\mathrm{B}}l_{\mathrm{B}}l'_{B}}$ is given by

$$\zeta^{L_{\mathrm{A}}L_{\mathrm{B}}L}_{l_{\mathrm{A}}l'_{\mathrm{A}}l_{\mathrm{B}}l'_{\mathrm{B}}} = (-1)^{l_{\mathrm{A}}+l'_{\mathrm{A}}} \left[\frac{(2l_{\mathrm{A}}+2l_{\mathrm{B}}+1)!(2l'_{\mathrm{A}}+2l'_{\mathrm{B}}+1)!}{(2l_{\mathrm{A}})!(2l_{\mathrm{B}})!(2l'_{\mathrm{A}})!(2l'_{\mathrm{B}})!}\right]^{1/2}$$
$$\times [L_{\mathrm{A}}, L_{\mathrm{B}}, L]^{1/2} \langle l_{\mathrm{A}}+l_{\mathrm{B}}, 0; l'_{\mathrm{A}}+l'_{\mathrm{B}}, 0 | L, 0\rangle, \tag{28}$$

where $[l_1, l_2, \ldots, l_n] = (2l_1+1)(2l_2+1)\ldots(2l_n+1)$.

We will frequently use the following equations,

$$\left(\frac{\partial Q_m^l}{\partial F^{m'}}\right)_{\mathbf{F}=\mathbf{0}} = \sum_{\lambda,\mu} \langle l, m; 1, m' \mid \lambda, \mu\rangle \, \alpha_\mu^{(l1)\lambda}(0), \tag{29}$$

$$\left(\frac{\partial \alpha_\mu^{(l_1 l_2)\lambda}(\omega)}{\partial F^{m'}}\right)_{\mathbf{F}=\mathbf{0}} = \sum_{\lambda',\mu'} \langle \lambda, \mu; 1, m' \mid \lambda', \mu'\rangle \, \beta_{\mu'}^{((l_1 l_2)\lambda 1)\lambda'}(\omega, 0), \tag{30}$$

$$\left(\frac{\partial^2 \alpha_\mu^{(l_1 l_2)\lambda}(\omega)}{\partial F^{m'} \partial F^{m''}}\right)_{\mathbf{F}=\mathbf{0}} = \sum_{\lambda',\mu'} \sum_{\lambda'',\mu''} \langle \lambda, \mu; 1, m' \mid \lambda', \mu'\rangle \langle \lambda', \mu'; 1, m'' \mid \lambda'', \mu''\rangle \times \gamma_{\mu''}^{(((l_1 l_2)\lambda 1)\lambda' 1)\lambda''}(\omega, 0, 0), \tag{31}$$

where $\beta_{\mu'}^{((ll')\lambda l'')\lambda'}(\omega, \omega')$ and $\gamma_{\mu'}^{(((l_1 l_2)ll')\lambda l'')\lambda'}(\omega, \omega', \omega'')$ are the irreducible components of the first and second frequency-dependent hyperpolarizability tensors obtained by successive Clebsch–Gordan coupling in the order indicated by the parentheses in the superscripts. Their reducible counterparts are, for instance, given in [70]. The derivatives $\partial/\partial F^m$ are cogredient to F_m, i.e.,

$$\begin{aligned} \frac{\partial}{\partial F^1} &= -\frac{1}{\sqrt{2}}\left(\frac{\partial}{\partial F_x} + i\frac{\partial}{\partial F_y}\right) \\ \frac{\partial}{\partial F^0} &= \frac{\partial}{\partial F_z} \\ \frac{\partial}{\partial F^{-1}} &= \frac{1}{\sqrt{2}}\left(\frac{\partial}{\partial F_x} - i\frac{\partial}{\partial F_y}\right). \end{aligned} \tag{32}$$

3.1. *The multipole expansion of the interaction-induced dipole moment*

By applying equations (29) and (30) to the asymptotic expressions for $E_{\text{pol}}^{(k)}$, equations (25)–(27), one can show that the contribution from the kth-order polarization term $E_{\text{pol}}^{(k)}$ to $\Delta\mu_m$, denoted as $\Delta\mu_{m,\text{pol}}^{(k)}$, can be written in terms of the complete orthogonal set of angular functions given in equation (23) and labelled by $\{\Lambda\} = \{L_A, K_A, L_B, K_B, L\}$, λ and m,

$$\Delta\mu_{m,\text{pol}}^{(k)} = \frac{1}{\sqrt{3}} \sum_{\{\Lambda\}} \sum_{\lambda} d_{\text{pol},\{\Lambda\}\lambda}^{(k)}(R) \, A_{\{\Lambda\}m}^{(\lambda)1}(\boldsymbol{\omega}_A, \boldsymbol{\omega}_B, \hat{\mathbf{R}}). \tag{33}$$

The radial expansion coefficients $d_{\text{pol},\{\Lambda\}\lambda}^{(k)}(R)$ in equation (33) can be written exclusively in terms of multipole moments and (hyper)polarizabilities. In particular, the radial part of the electrostatic contribution to $\Delta\mu_m$ in the multipole approximation can be written as

$$d_{\text{pol},\{\Lambda\}\lambda}^{(1)}(R) = R^{-(L+1)}(1 + (-1)^{L_A+L_B+L+\lambda}\hat{\mathscr{P}}_{AB})\,(-1)^{L_A}[L_A, L, \lambda]^{1/2} \times \binom{2L}{2L_B}^{1/2} \begin{Bmatrix} L_A & L_B & \lambda \\ L & 1 & L-L_B \end{Bmatrix} \alpha_{K_A}^{(L-L_B,1)L_A}(0)\, Q_{K_B}^{L_B}, \tag{34}$$

where the quantity between curly braces is a 6j symbol [90]. We see that the first-order

polarization contribution $\Delta\mu^{(1)}_{m,\mathrm{pol}}$ is due to the polarization of A by the electric field created by the permanent multipole moments on B, and vice versa.

If we denote the set of indices $\{l_\mathrm{A}, l'_\mathrm{A}, l_\mathrm{B}, l'_\mathrm{B}\}$ by $\{l\}$, the radial components of the induction contributions to the interaction-induced dipole in the multipole approximation can be written as

$$d^{(2)}_{\mathrm{ind},\{\Lambda\}\lambda}(R) = (-1)^{L_\mathrm{A}+L_\mathrm{B}+L} \sum_{\{l\}} R^{-(l_\mathrm{A}+l'_\mathrm{A}+l_\mathrm{B}+l'_\mathrm{B}+2)} \zeta^{L_\mathrm{A}L_\mathrm{B}L}_{l_\mathrm{A}l'_\mathrm{A}l_\mathrm{B}l'_\mathrm{B}} (1+(-1)^{L_\mathrm{A}+L_\mathrm{B}+\lambda}\hat{\mathscr{P}}_\mathrm{AB})$$

$$\times \left(\sum_{\lambda_\mathrm{A}} (-1)^{l_\mathrm{A}+\lambda_\mathrm{A}} [\lambda, \lambda_\mathrm{A}]^{1/2} \begin{Bmatrix} l_\mathrm{A} & l_\mathrm{B} & L_\mathrm{B} & \lambda \\ l_\mathrm{A}+l_\mathrm{B} & l'_\mathrm{B} & L_\mathrm{A} & 1 \\ L & l'_\mathrm{A}+l'_\mathrm{B} & l'_\mathrm{A} & \lambda_\mathrm{A} \end{Bmatrix} \right.$$

$$\times [\boldsymbol{\alpha}^{(l_\mathrm{A}1)\lambda_\mathrm{A}}(0) \otimes \mathbf{Q}^{l'_\mathrm{A}}]^{L_\mathrm{A}}_{K_\mathrm{A}} \alpha^{(l_\mathrm{B}l'_\mathrm{B})L_\mathrm{B}}_{K_B}(0)$$

$$\left. -\frac{1}{2} \sum_{\lambda_\mathrm{A}} [\lambda, \lambda_\mathrm{A}]^{1/2} \begin{Bmatrix} L_\mathrm{A} & L_\mathrm{B} & \lambda \\ L & 1 & \lambda_\mathrm{A} \end{Bmatrix} \begin{Bmatrix} l_\mathrm{A} & l'_\mathrm{A} & \lambda_\mathrm{A} \\ l_\mathrm{B} & l'_\mathrm{B} & L_\mathrm{B} \\ l_\mathrm{A}+l_\mathrm{B} & l'_\mathrm{A}+l'_\mathrm{B} & L \end{Bmatrix} \right.$$

$$\left. \times \beta^{((l_\mathrm{A}l'_\mathrm{A})\lambda_\mathrm{A}1)L_\mathrm{A}}_{K_\mathrm{A}}(0,0) [\mathbf{Q}^{l_\mathrm{B}} \otimes \mathbf{Q}^{l'_\mathrm{B}}]^{L_\mathrm{B}}_{K_\mathrm{B}} \right), \tag{35}$$

where the first quantity between curly braces denotes a $12j$ symbol of the first kind [91]. This can be written as a single sum of products of four $6j$ symbols, see appendix A. Note that the second-order induction dipole $\Delta\mu^{(2)}_{m,\mathrm{ind}}$ is caused by two different mechanisms. In the first mechanism a permanent moment on A induces a moment on B, which in turn induces a dipole on A (and vice versa). In the second mechanism, system A is polarized by two electric fields created by two permanent moments on B, and vice versa. This nonlinear effect requires a non-vanishing first hyperpolarizability on A (and B).

The dispersion contribution to the interaction induced dipole is

$$d^{(2)}_{\mathrm{disp},\{\Lambda\}\lambda}(R) = (-1)^{L_\mathrm{A}+L_\mathrm{B}+L+1} \sum_{\{l\}} R^{-(l_\mathrm{A}+l'_\mathrm{A}+l_\mathrm{B}+l'_\mathrm{B}+2)} \zeta^{L_\mathrm{A}L_\mathrm{B}L}_{l_\mathrm{A}l'_\mathrm{A}l_\mathrm{B}l'_\mathrm{B}} (1+(-1)^{L_\mathrm{A}+L_\mathrm{B}+\lambda}\hat{\mathscr{P}}_\mathrm{AB})$$

$$\times \sum_{\lambda_\mathrm{A}} [\lambda, \lambda_\mathrm{A}]^{1/2} \begin{Bmatrix} L_\mathrm{A} & L_\mathrm{B} & \lambda \\ L & 1 & \lambda_\mathrm{A} \end{Bmatrix} \begin{Bmatrix} l_\mathrm{A} & l'_\mathrm{A} & \lambda_\mathrm{A} \\ l_\mathrm{B} & l'_\mathrm{B} & L_\mathrm{B} \\ l_\mathrm{A}+l_\mathrm{B} & l'_\mathrm{A}+l'_\mathrm{B} & L \end{Bmatrix}$$

$$\times \frac{1}{2\pi} \int_0^\infty \beta^{((l_\mathrm{A}l'_\mathrm{A})\lambda_\mathrm{A}1)L_\mathrm{A}}_{K_\mathrm{A}}(i\omega, 0)\, \alpha^{(l_\mathrm{B}l'_\mathrm{B})L_\mathrm{B}}_{K_\mathrm{B}}(i\omega)\, \mathrm{d}\omega, \tag{36}$$

where the algebraic coefficients $\zeta^{L_\mathrm{A}L_\mathrm{B}L}_{l_\mathrm{A}l'_\mathrm{A}l_\mathrm{B}l'_\mathrm{B}}$ are given by equation (28).

Equations (34)–(36) can be simplified further by considering the molecular symmetry groups of the monomers A and B. For instance, if A is a diatom in a Σ state, only irreducible tensors with total magnetic quantum number $K_\mathrm{A} = 0$ are non-vanishing. If B is an atom in an S state only irreducible tensors with $L_\mathrm{B} = 0$ survive. In systems with inversion symmetry in a *gerade* state the sum of the orders of the multipole operators must be even; this gives, for example, the requirement that $l_1 + l_2 + 1$

must be even in order that the hyperpolarizability $\beta_{\mu}^{((l_1 l_2)\lambda 1)\lambda'}$ is non-zero. Thus we have for H_2–He:

$$K_A = L_B = K_B = 0, \quad \lambda = L_A, \quad L_A - \text{even}, \quad L - \text{odd}. \tag{37}$$

By substituting conditions (37) into equation (23), one finds that the angular function $A^{(\lambda)1}_{\{A\}m}(\boldsymbol{\omega}_A, \boldsymbol{\omega}_B, \hat{\mathbf{R}})$ reduces to

$$A_{L_A L m}(\hat{\mathbf{r}}, \hat{\mathbf{R}}) = [\mathbf{C}^{L_A}(\hat{\mathbf{r}}) \otimes \mathbf{C}^{L}(\hat{\mathbf{R}})]^1_m, \tag{38}$$

where $\hat{\mathbf{r}}$ is a unit vector along the axis of the diatom. Further simplification of equation (38) is obtained by assuming that $\hat{\mathbf{R}}$ lies along the z axis. Using $C^L_M(0,0) = \delta_{M,0}$, we obtain

$$A_{L_A L m}(\hat{\mathbf{r}}) = \langle L_A, m; L, 0 \,|\, 1, m \rangle \, C^{L_A}_m(\hat{\mathbf{r}}). \tag{39}$$

The radial electrostatic function is given by

$$d^{(1)}_{\text{pol}, L_A L}(R) = \delta_{L, L_A+1} \, R^{-(L_A+2)} \, [(2L_A+1)(L_A+1)(2L_A+3)]^{1/2} \, Q_0^{L_A} \, \alpha_0, \tag{40}$$

where $\alpha_0 = -\sqrt{\frac{1}{3}}\alpha^{(11)0}(0)$ denotes the static polarizability of the atom. The induction term can be written as

$$\begin{aligned} d^{(2)}_{\text{ind}, L_A L}(R) = \sum_{\{l\}} R^{-(l_A + l'_A + l_B + l'_B + 2)} \, \zeta^{L_A 0 L}_{l_A l'_A l_B l'_B} \\ \times \Bigg(- \sum_{\lambda_A} \delta_{l_B l'_B} [\lambda_A]^{1/2} [l_B]^{-1/2} \begin{Bmatrix} l_A & l'_A & L \\ l'_A + l_B & l_A + l_B & l_B \end{Bmatrix} \begin{Bmatrix} L & l'_A & l_A \\ \lambda_A & 1 & L_A \end{Bmatrix} \\ \times [\boldsymbol{\alpha}^{(l_A 1)\lambda_A}(0) \otimes \mathbf{Q}^{l'_A}]^{L_A}_0 \alpha_0^{(l_B l_B)0}(0) \\ + \frac{1}{2} \begin{Bmatrix} l_A & l'_A & L_A \\ l_B & l'_B & 1 \\ l_A + l_B & l'_A + l'_B & L \end{Bmatrix} [\mathbf{Q}^{l_A} \otimes \mathbf{Q}^{l'_A}]^{L_A}_0 \, \beta_0^{((l_B l'_B)11)0}(0,0) \Bigg), \end{aligned} \tag{41}$$

where in the first term l_A is odd and both λ_A and l'_A are even, while in the second term both l_A and l'_A are even, and $l_B + l'_B$ is odd. Finally, the dispersion term reads:

$$\begin{aligned} d^{(2)}_{\text{disp}, L_A L}(R) = - \sum_{\{l\}} R^{-(l_A + l'_A + l_B + l'_B + 2)} \zeta^{L_A 0 L}_{l_A l'_A l_B l'_B} \Bigg(\delta_{l_B l'_B} [l_B, L]^{-1/2} \\ \times \begin{Bmatrix} l_A & l'_A & L \\ l'_A + l_B & l_A + l_B & l_B \end{Bmatrix} \frac{1}{2\pi} \int_0^\infty \beta_0^{((l_A l'_A)L1)L_A}(i\omega, 0) \, \alpha_0^{(l_B l_B)0}(i\omega) \, \mathrm{d}\omega \\ + \begin{Bmatrix} l_A & l'_A & L_A \\ l_B & l'_B & 1 \\ l_A + l_B & l'_A + l'_B & L \end{Bmatrix} \frac{1}{2\pi} \int_0^\infty \alpha_0^{(l_A l'_A)L_A}(i\omega) \, \beta_0^{((l_B l'_B)11)0}(i\omega, 0) \, \mathrm{d}\omega \Bigg), \end{aligned} \tag{42}$$

where in the first term $l_A + l'_A$ is odd, and in the second term $l_A + l'_A$ is even and $l_B + l'_B$ is odd.

3.2. *The multipole expansion of the interaction-induced polarizabilities*

The contribution from the kth-order polarization term $E^{(k)}_{\rm pol}$ to $\Delta\alpha^{(11)l}_m$, denoted as $(\Delta\alpha^{(11)l}_m)^{(k)}_{\rm pol}$, can be written in terms of the orthogonal set of angular functions labelled by $\{\Lambda\} = \{L_{\rm A}, K_{\rm A}, L_{\rm B}, K_{\rm B}, L\}$, λ, l, and m, cf. equation (23),

$$(\Delta\alpha^{(11)l}_m)^{(k)}_{\rm pol} = \sum_{\{\Lambda\}} \sum_{\lambda} p^{(k)}_{{\rm pol},\{\Lambda\}\lambda l}(R)\, A^{\lambda l}_{\{\Lambda\}m}(\boldsymbol{\omega}_{\rm A}, \boldsymbol{\omega}_{\rm B}, \hat{\mathbf{R}}), \tag{43}$$

where $l = 0, 2$.

Similarly as in the case of the dipole moments, the final formulas for the interaction-induced polarizabilities can be expressed solely in terms of multipole moments and (hyper)polarizabilities. For instance, the electrostatic contribution to $\Delta\alpha^{(11)l}_m$ in the multipole approximation can be written as

$$\begin{aligned} p^{(1)}_{{\rm pol},\{\Lambda\}\lambda l}(R) = {} & R^{-(L+1)}(1+(-1)^{L_{\rm A}+L_{\rm B}+L+\lambda}\hat{\mathscr{P}}_{\rm AB}) \\ & \times \Bigg(\Big(\sum_{\lambda_{\rm A}\lambda_{\rm B}} (-1)^{\lambda_{\rm A}+1} \delta_{{\rm L},\lambda_{\rm A}+\lambda_{\rm B}}\, \alpha^{(\lambda_{\rm A}1)L_{\rm A}}_{K_{\rm A}}(0)\, \alpha^{(\lambda_{\rm B}1)L_{\rm B}}_{K_{\rm B}}(0) \begin{pmatrix} 2L \\ 2\lambda_{\rm A} \end{pmatrix}^{1/2} \\ & \times [L_{\rm A}, L_{\rm B}, L, \lambda]^{1/2} \begin{Bmatrix} L_{\rm A} & L_{\rm B} & \lambda \\ \lambda_{\rm A} & \lambda_{\rm B} & L \\ 1 & 1 & l \end{Bmatrix} \\ & + \sum_{\lambda_{\rm A}} (-1)^{L_{\rm B}+L+1} \beta^{((L-L_{\rm B},1)\lambda_{\rm A}1)L_{\rm A}}_{K_{\rm A}}(0,0)\, Q^{L_{\rm B}}_{K_{\rm B}} \begin{pmatrix} 2L \\ 2L_{\rm B} \end{pmatrix}^{1/2} \\ & \times [L_{\rm A}, L, \lambda_{\rm A}, \lambda]^{1/2} \begin{Bmatrix} L-L_{\rm B} & l & L_{\rm A} \\ 1 & \lambda_{\rm A} & 1 \end{Bmatrix} \begin{Bmatrix} L_{\rm A} & \lambda & L_{\rm B} \\ L & L-L_{\rm B} & l \end{Bmatrix} \Bigg) . \end{aligned} \tag{44}$$

The multipole-expanded formula for the induction contribution to the interaction-induced polarizabilities is more involved, and can be conveniently expressed as,

$$\begin{aligned} p^{(2)}_{{\rm ind},\{\Lambda\}\lambda l}(R) = \sum_{\{l\}} {} & R^{-(l_{\rm A}+l'_{\rm A}+l_{\rm B}+l'_{\rm B}+2)} \zeta^{L_{\rm A}L_{\rm B}L}_{l_{\rm A}l'_{\rm A}l_{\rm B}l'_{\rm B}} (1+(-1)^{L_{\rm A}+L_{\rm B}+\lambda}\hat{\mathscr{P}}_{\rm AB}) \\ & \times \Bigg(\sum_{\lambda_{\rm A}\lambda'_{\rm A}} \xi_{\rm I}\, \gamma^{(((l_{\rm A}l'_{\rm A})\lambda_{\rm A}1)\lambda'_{\rm A}1)L_{\rm A}}_{K_{\rm A}}(0,0,0)\, [\mathbf{Q}^{l_{\rm B}} \otimes \mathbf{Q}^{l'_{\rm B}}]^{L_{\rm B}}_{K_{\rm B}} \\ & + \sum_{\lambda_{\rm A}\lambda_{\rm B}} \xi_{\rm II}\, \beta^{((l_{\rm A}l'_{\rm A})\lambda_{\rm A}1)L_{\rm A}}_{K_{\rm A}}(0,0)\, [\boldsymbol{\alpha}^{(l_{\rm B}1)\lambda_{\rm B}}(0) \otimes \mathbf{Q}^{l'_{\rm B}}]^{L_{\rm B}}_{K_{\rm B}} \\ & + \sum_{\lambda_{\rm B}\lambda'_{\rm B}} \xi_{\rm III}\, \alpha^{(l_{\rm A}l'_{\rm A})L_{\rm A}}_{K_{\rm A}}(0)\, [\boldsymbol{\beta}^{((l_{\rm B}1)\lambda_{\rm B}1)\lambda'_{\rm B}}(0,0) \otimes \mathbf{Q}^{l'_{\rm B}}]^{L_{\rm B}}_{K_{\rm B}} \\ & + \sum_{\lambda_{\rm B}\lambda'_{\rm B}} \xi_{\rm IV}\, \alpha^{(l_{\rm A}l'_{\rm A})L_{\rm A}}_{K_{\rm A}}(0)\, [\boldsymbol{\alpha}^{(l_{\rm B}1)\lambda_{\rm B}}(0) \otimes \boldsymbol{\alpha}^{(l'_{\rm B}1)\lambda'_{\rm B}}(0)]^{L_{\rm B}}_{K_{\rm B}} \Bigg), \end{aligned} \tag{45}$$

with the algebraic coefficients ξ given by,

$$\xi_{\mathrm{I}} = \tfrac{1}{2}(-1)^{L_B+L+\lambda_A}[\lambda_A, \lambda'_A, \lambda]^{1/2} \begin{Bmatrix} l_A & l'_A & \lambda_A \\ l_B & l'_B & L_B \\ l_A+l_B & l'_A+l'_B & L \end{Bmatrix} \begin{Bmatrix} 1 & \lambda_A & \lambda'_A \\ L_A & 1 & l \end{Bmatrix} \begin{Bmatrix} l & L & \lambda \\ L_B & L_A & \lambda_A \end{Bmatrix}, \tag{46}$$

$$\xi_{\mathrm{II}} = 2[\lambda_A, \lambda_B, \lambda]^{1/2} \begin{Bmatrix} L_A & l'_A & L_B & l'_B & \lambda & l'_A+l'_B \\ \lambda_A & & \lambda_B & & L & \\ 1 & l_A & 1 & l_B & l & l_A+l_B \end{Bmatrix}, \tag{47}$$

$$\xi_{\mathrm{III}} = (-1)^{L+\lambda}[\lambda_B, \lambda'_B, \lambda]^{1/2} \begin{Bmatrix} L_A & l_A & l_B & \lambda'_B \\ l'_A & l_A+l_B & l & L_B \\ l'_B & l'_A+l'_B & L & \lambda \end{Bmatrix} \begin{Bmatrix} \lambda'_B & l_B & l \\ 1 & 1 & \lambda_B \end{Bmatrix}, \tag{48}$$

$$\xi_{\mathrm{IV}} = (-1)^{L_A+L_B+L}[\lambda_B, \lambda'_B, \lambda]^{1/2} \begin{Bmatrix} l'_A & \lambda'_B & L_A & L_B & l_A & \lambda_B \\ & l'_B & & \lambda & & l_B \\ l'_A+l'_B & 1 & L & l & l_A+l_B & 1 \end{Bmatrix}, \tag{49}$$

where the symbol between curly braces occurring in equation (47) and (49) denotes a $15j$ symbol of the third kind (see appendix A for its definition). Finally, the multipole-expanded formula for the dispersion contribution to the interaction induced polarizabilities can be expressed as

$$p^{(2)}_{\mathrm{disp},\{\Lambda\}\lambda l}(R) = \sum_{\{l\}} R^{-(l_A+l'_A+l_B+l'_B+2)} \zeta^{L_A L_B L}_{l_A l'_A l_B l'_B} (1+(-1)^{L_A+L_B+\lambda}\hat{\mathscr{P}}_{AB})$$
$$\times \left(\sum_{\lambda_A \lambda'_A} \xi_{\mathrm{I}} \frac{1}{\pi} \int_0^\infty \gamma^{(((l_A l'_A)\lambda_A 1)\lambda'_A 1)L_A}_{K_A}(i\omega, 0, 0)\, \alpha^{(l_B l'_B)L_B}_{K_B}(i\omega)\, \mathrm{d}\omega \right.$$
$$\left. + \sum_{\lambda_A \lambda_B} \xi_{\mathrm{V}} \frac{1}{\pi} \int_0^\infty \beta^{((l_A l'_A)\lambda_A 1)L_A}_{K_A}(i\omega, 0)\, \beta^{((l_B l'_B)\lambda_B 1)L_B}_{K_B}(i\omega, 0)\, \mathrm{d}\omega \right), \tag{50}$$

where ξ_{I} is given by equation (46) and ξ_{V} is defined as,

$$\xi_{\mathrm{V}} = \tfrac{1}{2}[\lambda_A, \lambda_B, \lambda]^{1/2} \begin{Bmatrix} l_A & l'_A & \lambda_A \\ l_B & l'_B & \lambda_B \\ l_A+l_B & l'_A+l'_B & L \end{Bmatrix} \begin{Bmatrix} L_A & L_B & \lambda \\ \lambda_A & \lambda_B & L \\ 1 & 1 & l \end{Bmatrix}. \tag{51}$$

If A and B are identical atoms in the same S state, the multipole expressions reported above are simplified drastically, since in this particular case we have

$$L_A = K_A = L_B = K_B = \lambda = m = 0, \quad L = l. \tag{52}$$

Taking further the z axis along **R**, so that the angular function $A^{0l}_{\{0,0,0,0,l\}m} = \delta_{m0}$, we find that the electrostatic functions are given by the following expressions, cf. also equations (43) and (44),

$$(\Delta\alpha_0^{(11)0})^{(1)}_{\mathrm{pol}} = 0, \tag{53}$$

$$(\Delta\alpha_0^{(11)2})^{(1)}_{\mathrm{pol}} = 2\sqrt{6}R^{-3}(\alpha_0)^2. \tag{54}$$

In some applications it is more convenient to use the trace polarizability $\alpha \equiv (\Delta\alpha_{zz}+2\Delta\alpha_{xx})/3$ and the anisotropy $\Delta\alpha_{zz}-\Delta\alpha_{xx}$. These are related to the components $\Delta\alpha_0^{(11)0}$ and $\Delta\alpha_0^{(11)2}$ by the equations

$$\alpha = -\frac{1}{\sqrt{3}}\Delta\alpha_0^{(11)0}, \quad \Delta\alpha_{zz}-\Delta\alpha_{xx} = \tfrac{1}{2}\sqrt{6}\Delta\alpha_0^{(11)2}. \tag{55}$$

Equation (53) shows that the electrostatic contribution to the interaction-induced polarizability of two identical atoms is traceless in the multipole approximation. This relation generally holds for any complex consisting of two atoms in S states.

The induction term can be written as,

$$(\Delta\alpha_0^{(11)l})_{\mathrm{ind}}^{(2)}(R) = 2\sum_{l'}(-1)^{l'} R^{-(2l'+4)}(2l'+1)(l'+1)(2l'+3)(\alpha_0)^2\alpha_{l'}(0)$$
$$\times\langle l'+1,0;l'+1,0\,|\,l,0\rangle\begin{Bmatrix} l'+1 & l'+1 & l \\ 1 & 1 & l'\end{Bmatrix}, \tag{56}$$

where $\alpha_{l'}(0) = (-1)^{l'}[l']^{-1/2}\alpha_0^{(l'l')0}$ is the static $2^{l'}$-pole polarizability of the atom. The dispersion term reads:

$$(\Delta\alpha_0^{(11)l})_{\mathrm{disp}}^{(2)}(R) = \sum_{\{l\}} R^{-(l_{\mathrm{A}}+l'_{\mathrm{A}}+l_{\mathrm{B}}+l'_{\mathrm{B}}+2)}\langle l_{\mathrm{A}}+l_{\mathrm{B}},0;l'_{\mathrm{A}}+l'_{\mathrm{B}},0\,|\,l,0\rangle$$
$$\times\left[\frac{(2l_{\mathrm{A}}+2l_{\mathrm{B}}+1)!(2l'_{\mathrm{A}}+2l'_{\mathrm{B}}+1)!}{(2l_{\mathrm{A}})!(2l_{\mathrm{B}})!(2l'_{\mathrm{A}})!(2l'_{\mathrm{B}})!}\right]^{1/2}$$
$$\times\Bigg(\delta_{l_{\mathrm{B}},l'_{\mathrm{B}}}[l_{\mathrm{B}},l]^{-1/2}\begin{Bmatrix} l_{\mathrm{A}}+l_{\mathrm{B}} & l'_{\mathrm{A}}+l_{\mathrm{B}} & l \\ l'_{\mathrm{A}} & l_{\mathrm{A}} & l_{\mathrm{B}}\end{Bmatrix}$$
$$\times\frac{1}{\pi}\int_0^\infty \gamma_0^{(((l_{\mathrm{A}}l'_{\mathrm{A}})l1)11)0}(i\omega,0,0)\,\alpha_0^{(l_{\mathrm{B}}l_{\mathrm{B}})0}(i\omega)\,\mathrm{d}\omega$$
$$-\begin{Bmatrix} l_{\mathrm{A}} & l'_{\mathrm{A}} & 1 \\ l_{\mathrm{B}} & l'_{\mathrm{B}} & 1 \\ l_{\mathrm{A}}+l_{\mathrm{B}} & l'_{\mathrm{A}}+l'_{\mathrm{B}} & l\end{Bmatrix}\frac{1}{\pi}\int_0^\infty \beta_0^{((l_{\mathrm{A}}l'_{\mathrm{A}})11)0}(i\omega,0)\,\beta_0^{((l_{\mathrm{B}}l'_{\mathrm{B}})11)0}(i\omega,0)\,\mathrm{d}\omega\Bigg). \tag{57}$$

4. Computational details

The collision-induced dipole of He–H_2 and the collision-induced dipole polarizability of He_2 were computed from SAPT interaction energies. Calculations on He–H_2 were performed for several intermolecular distances R and angles ϑ, where **R** is the vector pointing from the centre of mass of H_2 to the He nucleus, and ϑ is the angle between the vectors **r**, pointing from one hydrogen atom to the other, and **R**. Computations on He_2 were performed for several interatomic distances R.

For the He atom in He–H_2 we used a [5s4p3d2f] basis. The s orbitals were represented by the (61111) contraction of Van Duijneveldt's 10s set [92], and the exponents of the polarization functions were taken from Gutowski *et al.* [93]. For H_2 we used a [4s3p2d1f] basis, where we took the s and p functions from Hobza *et al.* [94], and the d and f functions from basis D of Williams *et al.* [75]. For the helium atom in He_2 we used a larger [7s5p4d3f2g] basis. The s orbitals were again represented by the 10s set of [92], now contracted to (4111111) and the exponents of the polarization functions were taken from [93]. To check the convergence of the SAPT expansion by comparison with full CI (FCI) results, we performed additional calculations in smaller basis sets. For the He atom in He–H_2 we used a [5s3p1d] basis, where the s functions are the same as in the larger basis and the polarization functions were again taken from [93]. (The 3p set was represented by the optimal even-tempered basis.) For H_2 we used a [3s1p; 3s2p1d] basis, including bond functions at the centre of the molecule. The s

and p functions were taken from Meyer *et al.* [14], while we assigned the value 0·3 to the exponent of the d functions, as suggested in [94]. For the FCI computations on He_2 we used a [5s3p2d] basis, where the s and p functions are the same as in He–H_2 and the d functions were taken from [93]. The spherical form of the polarization functions has been used (5 d functions and 7 f functions). In order to account fully for the charge-overlap effects all calculations have been performed using the full dimer basis set.

All calculations of interaction energies have been performed with the SAPT system of codes [95]. In addition, FCI results have been obtained from the program by Zarrabian *et al.* [96]. We used the Boys–Bernardi counterpoise correction to eliminate the basis set superposition error from the supermolecular Hartree–Fock and FCI calculations [97]. The components of the interaction-induced dipole moment $\Delta\mu_i$ of He–H_2 and of the interaction-induced polarizability tensor $\Delta\alpha_{ii}$ of He_2 have been obtained from the equations

$$\Delta\mu_i = -\frac{E_{\text{int}}(F_i) - E_{\text{int}}(-F_i)}{2F_i} + O(F_i^3), \tag{58}$$

$$\Delta\alpha_{ii} = -\frac{E_{\text{int}}(F_i) + E_{\text{int}}(-F_i) - 2E_{\text{int}}(0)}{F_i^2} + O(F_i^4), \tag{59}$$

where the index $i = z$ or x denotes the direction along the intermolecular axis **R**, or perpendicular to this axis, respectively. Note that for He_2 only the diagonal components of the collision-induced polarizability tensor are non-zero. We used field strengths equal to $\pm 0{\cdot}001$ au in the calculations of the interaction-induced polarizability of He_2 and field strengths of $\pm 0{\cdot}0001$ au in the calculations of the interaction-induced dipole moment of He–H_2.

In addition, long-range van der Waals coefficients corresponding to the multipole-expanded electrostatic, induction, and dispersion contributions to the interaction-induced dipole moment of He–H_2 and polarizability of He_2 have been computed through R^{-11} and R^{-10}, respectively. We used the same level of theory and the same basis sets as in the SAPT calculations. The long-range electrostatic coefficients of equations (40) and (54) were calculated including intramolecular correlation up to and including third order. Zero-order multipole moments and polarizabilities were computed at the Hartree–Fock and coupled Hartree–Fock (CHF) levels of theory, respectively. The true correlation contributions to the moments and polarizabilities were calculated with the inclusion of coupled Hartree–Fock type response of the orbitals.

The long-range induction coefficients of equations (41) and (56) were calculated up to and including second order of true correlation. The zero-order multipole moments and (hyper)polarizabilities were computed at the Hartree–Fock and CHF levels, respectively. The second-order true correlation contributions to the moments and polarizabilities were obtained from the POLCOR package [71, 72] and the hyper-polarizabilities were obtained by differentiating the corresponding polarizabilities. Finally, the long-range dispersion coefficients of equations (42) and (57) were computed from dynamic (hyper)polarizabilities with both true and apparent correlation incorporated up to and including second order [76]. The correlation contributions to the polarizabilities were obtained from POLCOR and the hyper-polarizabilities by differentiation. The long-range induction and dispersion coefficients were calculated without the inclusion of coupled Hartree–Fock type response of the orbitals.

In the calculation of the hyperpolarizabilities by a finite field approach we used the following equations, which hold for S state atoms,

$$\beta_0^{((l_A l'_A)11)0}(\omega,0) = -\sqrt{3}\left(\frac{\partial \alpha_0^{(l_A l'_A)1}(\omega)}{\partial F^0}\right)_{F=0},$$

$$\gamma_0^{(((l_A l'_A)l1)11)0}(\omega,0,0) = \begin{pmatrix} l & 1 & 1 \\ 0 & 0 & 0 \end{pmatrix}^{-1} \left(\frac{\partial^2 \alpha_0^{(l_A l'_A)1}}{\partial F^0 \partial F^0}\right)_{F=0}. \tag{60}$$

See equations (56) and (57) and appendix B for the expressions used in the case of He_2 and equations (40)–(42) for the required He–H_2 expressions. We chose as the xz plane the mirror plane spanned by the H_2 axis and the external field. The H_2 irreducible components then satisfy

$$\alpha_M^{(ll')L} = (-1)^{l+l'+L+M} \alpha_{-M}^{(ll')L}. \tag{61}$$

The Casimir–Polder integrals occurring in equations (42) and (57) were computed on a 10 point grid as described in [98].

5. Numerical illustration

5.1. *Interaction-induced dipole moment of He–H_2*

As discussed in section 2, the symmetry-adapted perturbation theory in low orders provides the basis for understanding the mechanisms that yield the interaction-induced properties. However, the convergence of the SAPT expansion with respect to both the intermolecular interaction and the intramolecular electronic correlation must be fast enough to enable practical applications of *ansatz* (11) in the calculations of the collision-induced properties. Table 1 compares the components of the interaction-induced dipole moment of He–H_2 computed at the FCI level with the SAPT results in the same basis set. For each geometry of the complex considered in this table, SAPT recovers at least 94 % of the FCI results. The convergence rate of the SAPT expansion depends slightly on the intermolecular separation R. In the region of the van der Waals minimum our SAPT results recover more than 96 % of the FCI values. For smaller R the accuracy of SAPT deteriorates somewhat due to the increase in the strength of the perturbation. Although these calculations were performed in the small basis set of spd quality, we expect the error to be largely independent of the basis set. It is reasonable then to assume that the effect of the truncation of the perturbation series on the components of the interaction-induced dipole moment of He–H_2 should be smaller than 6 %.

The values of various contributions to the components of the interaction-induced dipole moment of He–H_2 are reported as function of the angle ϑ in tables 2 and 3 for two distances: 5 a_0 and 7 a_0, bracketing the minimum in the isotropic van der Waals potential which is at 6·42 a_0 [99] ($a_0 \approx 5{\cdot}29177 \times 10^{-11}$ m). See also figures 1–4 for graphical illustrations. An inspection of table 2 and figure 1 shows that at 5 a_0 the first-order exchange term is by far the largest contribution to the parallel component of the interaction-induced dipole. However, other terms are non-negligible, and the final anisotropy of the dipole surface results from the cancellation of large positive and negative contributions. By contrast, the ϑ dependence of the dipole surface for the perpendicular component is to a large extent determined by the sum $\Delta\mu_{x,\mathrm{pol}}^{(1)} + \Delta\mu_{x,\mathrm{exch}}^{(1)}$. Other contributions are relatively less important, and amount to 15 % of $\Delta\mu_x$. It is

Table 1. Comparison of the parallel component of the interaction-induced dipole moment of He–H_2 computed by SAPT with the FCI results (in 10^{-3} au). All results were computed in the [5s3p1d/3s1p; 3s2p1d] basis.

	$\vartheta = 0$			$\vartheta = 90°$		
	$R = 5\ a_0$	$R = 6{\cdot}5\ a_0$	$R = 10\ a_0$	$R = 5\ a_0$	$R = 7\ a_0$	$R = 10\ a_0$
SAPT	12·377	1·835	0·217	3·629	−0·318	−0·114
FCI	13·056	1·869	0·215	3·875	−0·306	−0·113
Δ^a	−5·2%	−1·8%	0·9%	−6·3%	3·9%	0·88%

[a] Relative error of the SAPT result with respect to the FCI result.

Table 2. SAPT contributions (in 10^{-3} au) to the parallel component of the interaction-induced dipole moment of He–H_2 as a function of the angle ϑ at $R = 5\ a_0$ and $7\ a_0$. The numbers in parentheses represent the intramonomer correlation contributions. The H—H distance is fixed at $1{\cdot}449\ a_0$. All results were computed in the [5s4p3d2f/4s3p2d1f] basis.

	$\vartheta = 0$		$\vartheta = 30°$		$\vartheta = 60°$		$\vartheta = 90°$	
$R = 5\ a_0$								
$\Delta\mu_{z,\mathrm{pol}}^{(1)}$	0·308	(−0·053)	−0·660	(+0·003)	−2·485	(+0·094)	−3·344	(+0·130)
$\Delta\mu_{z,\mathrm{exch}}^{(1)}$	15·840	(+0·018)	14·120	(−0·046)	11·202	(−0·137)	9·962	(−0·168)
$\Delta\mu_{z,\mathrm{ind}}^{(2)}$	−1·017	(+0·020)	−1·074	(+0·024)	−1·137	(+0·030)	−1·145	(+0·031)
$\Delta\mu_{z,\mathrm{exch\text{-}ind}}^{(2)}$	2·093		1·873		1·500		1·340	
$\Delta\mu_{z,\mathrm{disp}}^{(2)}$	−2·805		−2·524		−2·027		−1·811	
$\Delta\mu_{z,\mathrm{exch\text{-}disp}}^{(2)}$	0·433		0·387		0·307		0·272	
$\Delta\mu_z$	12·107		9·627		5·300		3·403	
$R = 7\ a_0$								
$\Delta\mu_{z,\mathrm{pol}}^{(1)}$	0·7727	(−0·0160)	0·4480	(−0·0079)	−0·1749	(+0·0072)	−0·4735	(+0·0142)
$\Delta\mu_{z,\mathrm{exch}}^{(1)}$	0·5244	(−0·0092)	0·4712	(−0·0099)	0·3811	(−0·0108)	0·3428	(−0·0111)
$\Delta\mu_{z,\mathrm{ind}}^{(2)}$	0·0057	(+0·0011)	−0·0078	(+0·0012)	−0·0290	(+0·0013)	−0·0369	(+0·0013)
$\Delta\mu_{z,\mathrm{exch\text{-}ind}}^{(2)}$	0·0451		0·0407		0·0331		0·0298	
$\Delta\mu_{z,\mathrm{disp}}^{(2)}$	−0·2727		−0·2478		−0·2030		−0·1833	
$\Delta\mu_{z,\mathrm{exch\text{-}disp}}^{(2)}$	0·0198		0·0179		0·0145		0·0130	
$\Delta\mu_z$	1·0297		0·6627		−0·0271		−0·3526	

interesting to note that among various post-Hartree–Fock contributions to $\Delta\mu_z$ and $\Delta\mu_x$, the intermonomer correlation, i.e., the sum of the dispersion and exchange–dispersion contributions, is dominant. The exchange quenching of the dispersion contribution is unexpectedly important, since it represents as much as 15% of $\Delta\mu_{z,\mathrm{disp}}^{(2)}$, and 12% of $\Delta\mu_{x,\mathrm{disp}}^{(2)}$. The intramonomer correlation contributions to $\Delta\mu_{i,\mathrm{pol}}^{(1)}$, $\Delta\mu_{i,\mathrm{exch}}^{(1)}$, and $\Delta\mu_{\mathrm{ind}}^{(2)}$ are negligibly small, and amount to a fraction of a per cent of $\Delta\mu_i$ at all angles. This suggests that the 'Hartree–Fock plus dispersion' model possibly could be applied in practice, provided that the dispersion contribution is not approximated by its multipole expansion (cf. the discussion below). These findings are in agreement with the supermolecule results of Meyer and Frommhold [16] from localized coupled electron pair approximation calculations.

At $7\ a_0$, just outside the isotropic van der Waals minimum, the first order electrostatic and exchange contributions are equally important for the parallel component, while the perpendicular component is dominated by the electrostatic contribution. At this distance $\Delta\mu_{z,\mathrm{pol}}^{(1)}$ is due mainly to the polarization of the He atom by the H_2 quadrupole, as is witnessed by the factor of about −2 between the values of $\vartheta = 0$ and 90°. Recall that the SAPT approach does not use the multipole expansion [68, 69], so that in the present calculations all charge overlap (damping) effects are fully

Table 3. SAPT contributions (in 10^{-3} au) to the perpendicular component of the interaction-induced dipole moment of He–H_2 as a function of the angle ϑ at $R = 5\ a_0$ and $7\ a_0$. The numbers in parentheses represent the intramonomer correlation contributions. The H—H distance is fixed at $1{\cdot}449\ a_0$. All results were computed in the [5s4p3d2f/4s3p2d1f] basis.

	$\vartheta = 30°$		$\vartheta = 45°$		$\vartheta = 60°$	
$R = 5\ a_0$						
$\Delta\mu_{x,\mathrm{pol}}^{(1)}$	−1·644	(+0·029)	−1·818	(+0·033)	−1·510	(+0·029)
$\Delta\mu_{x,\mathrm{exch}}^{(1)}$	0·770	(+0·025)	0·811	(+0·024)	0·642	(+0·016)
$\Delta\mu_{x,\mathrm{ind}}^{(2)}$	0·095	(−0·001)	0·096	(−0·000)	0·071	(−0·000)
$\Delta\mu_{x,\mathrm{exch-ind}}^{(2)}$	0·026		0·027		0·021	
$\Delta\mu_{x,\mathrm{disp}}^{(2)}$	−0·257		−0·282		−0·231	
$\Delta\mu_{x,\mathrm{exch-disp}}^{(2)}$	0·032		0·034		0·027	
$\Delta\mu_x$	−1·038		−1·196		−1·029	
$R = 7\ a_0$						
$\Delta\mu_{x,\mathrm{pol}}^{(1)}$	−0·3775	(+0·0083)	−0·4280	(+0·0094)	−0·3640	(+0·0079)
$\Delta\mu_{x,\mathrm{exch}}^{(1)}$	0·0178	(+0·0003)	0·0185	(+0·0003)	0·0144	(+0·0002)
$\Delta\mu_{x,\mathrm{ind}}^{(2)}$	0·0094	(−0·0001)	0·0094	(−0·0001)	0·0069	(−0·0000)
$\Delta\mu_{x,\mathrm{exch-ind}}^{(2)}$	0·0005		0·0005		0·0004	
$\Delta\mu_{x,\mathrm{disp}}^{(2)}$	−0·0244		−0·0271		−0·0225	
$\Delta\mu_{x,\mathrm{exch-disp}}^{(2)}$	0·0010		0·0010		0·0008	
$\Delta\mu_x$	−0·3745		−0·4268		−0·3649	

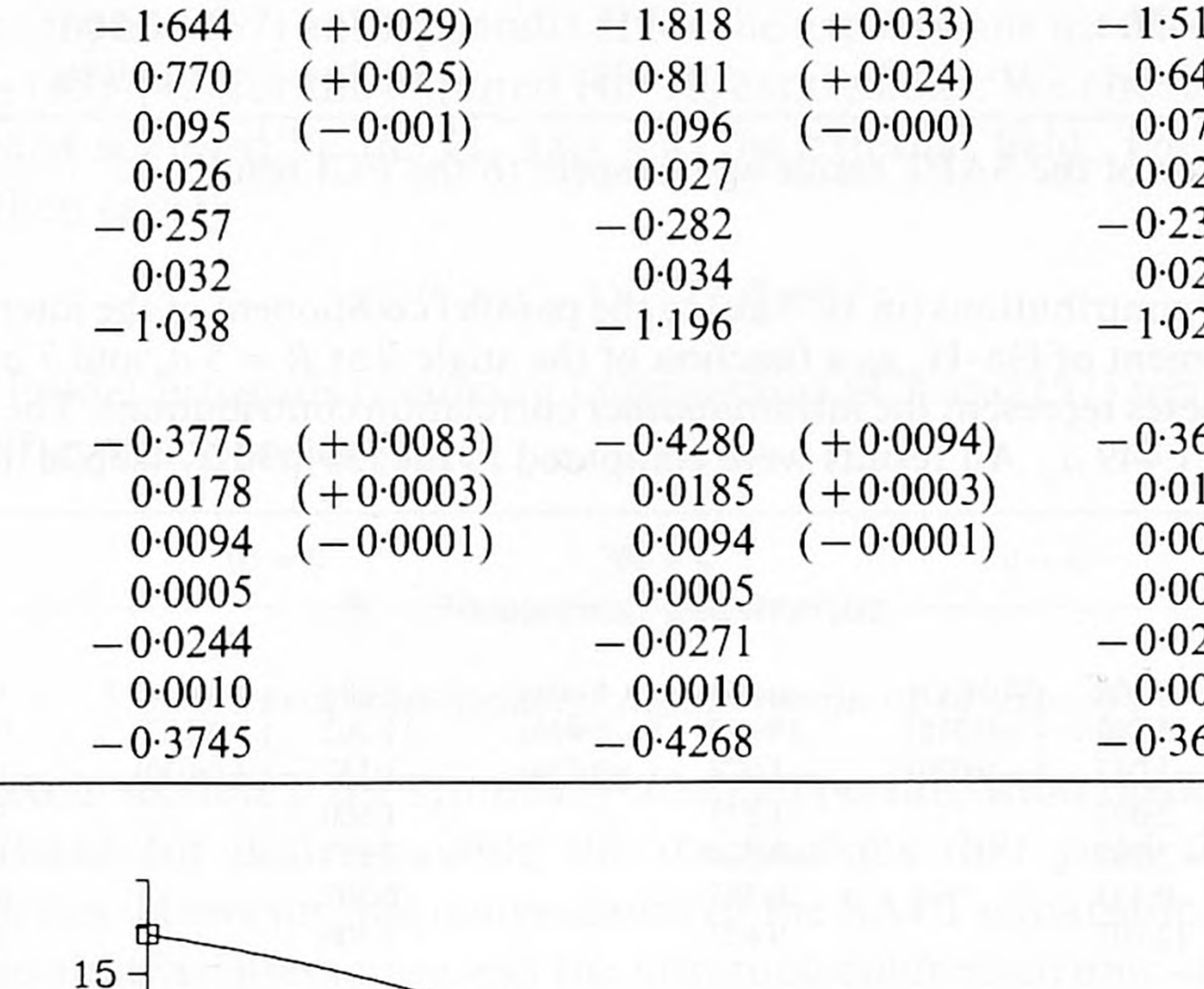

Figure 1. Comparison of the different SAPT contributions to the parallel component of the interaction-induced dipole moment of He–H_2 (in 10^{-3} au) as functions of the angle ϑ at $R = 5\ a_0$. The H—H distance is fixed at $1{\cdot}449\ a_0$. Open circles correspond to $\Delta\mu_{z,\mathrm{pol}}^{(1)}$, open squares to $\Delta\mu_{z,\mathrm{exch}}^{(1)}$, open triangles to $\Delta\mu_{z,\mathrm{ind}}^{(2)}$, diamonds to $\Delta\mu_{z,\mathrm{exch-ind}}^{(2)}$, crosses to $\Delta\mu_{z,\mathrm{disp}}^{(2)}$, filled triangles to $\Delta\mu_{z,\mathrm{exch-disp}}^{(2)}$ and filled circles to the sum value (dashed line).

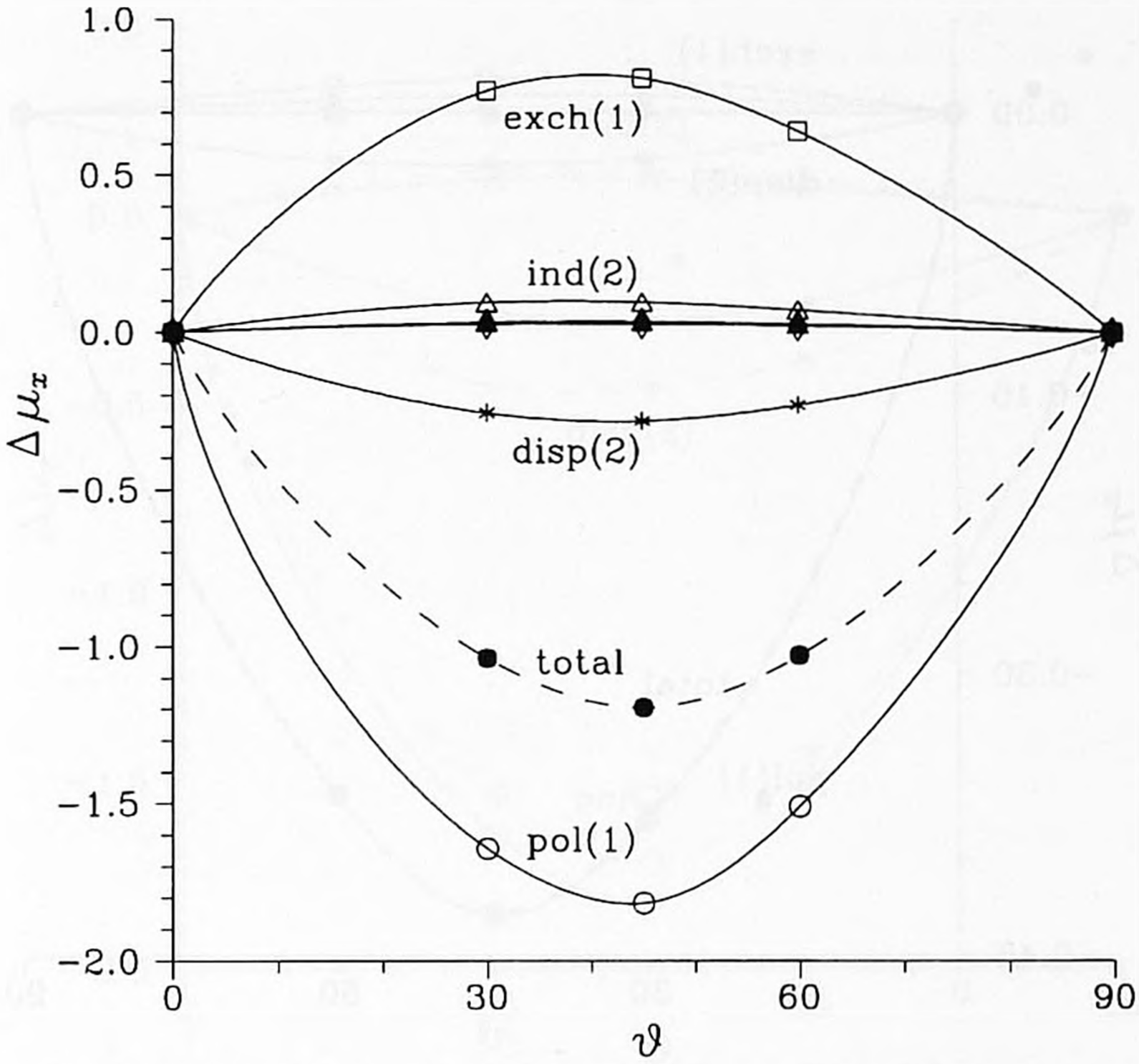

Figure 2. Comparison of the different SAPT contributions to the perpendicular component of the interaction-induced dipole moment of He–H_2 (in 10^{-3} au) as functions of the angle ϑ at $R = 5\ a_0$. The H—H distance is fixed at 1·449 a_0. Labels as for figure 1.

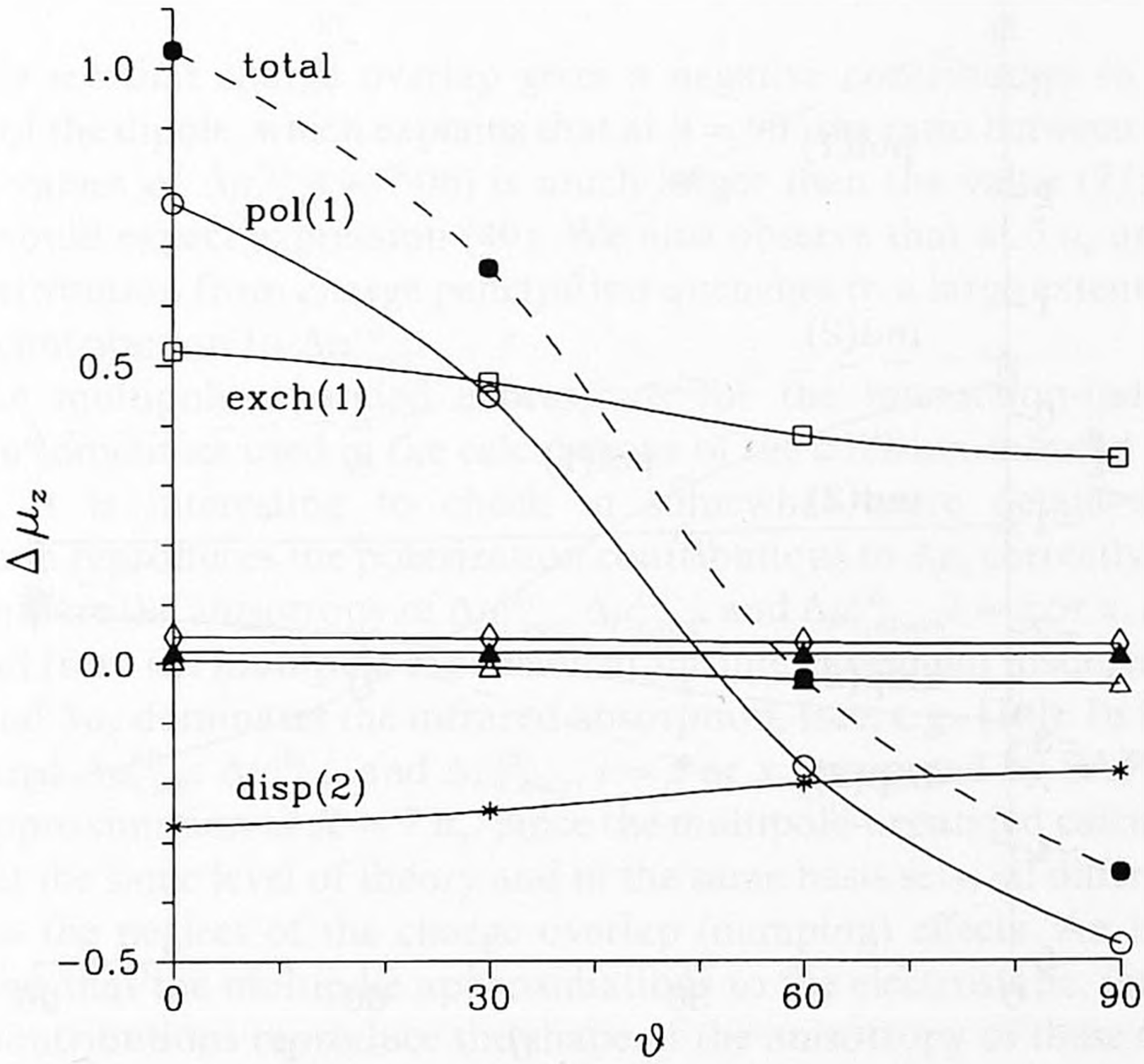

Figure 3. Comparison of the different SAPT contributions to the parallel component of the interaction-induced dipole moment of He–H_2 (in 10^{-3} au) as functions of the angle ϑ at $R = 7\ a_0$. The H—H distance is fixed at 1·449 a_0. Labels as for figure 1.

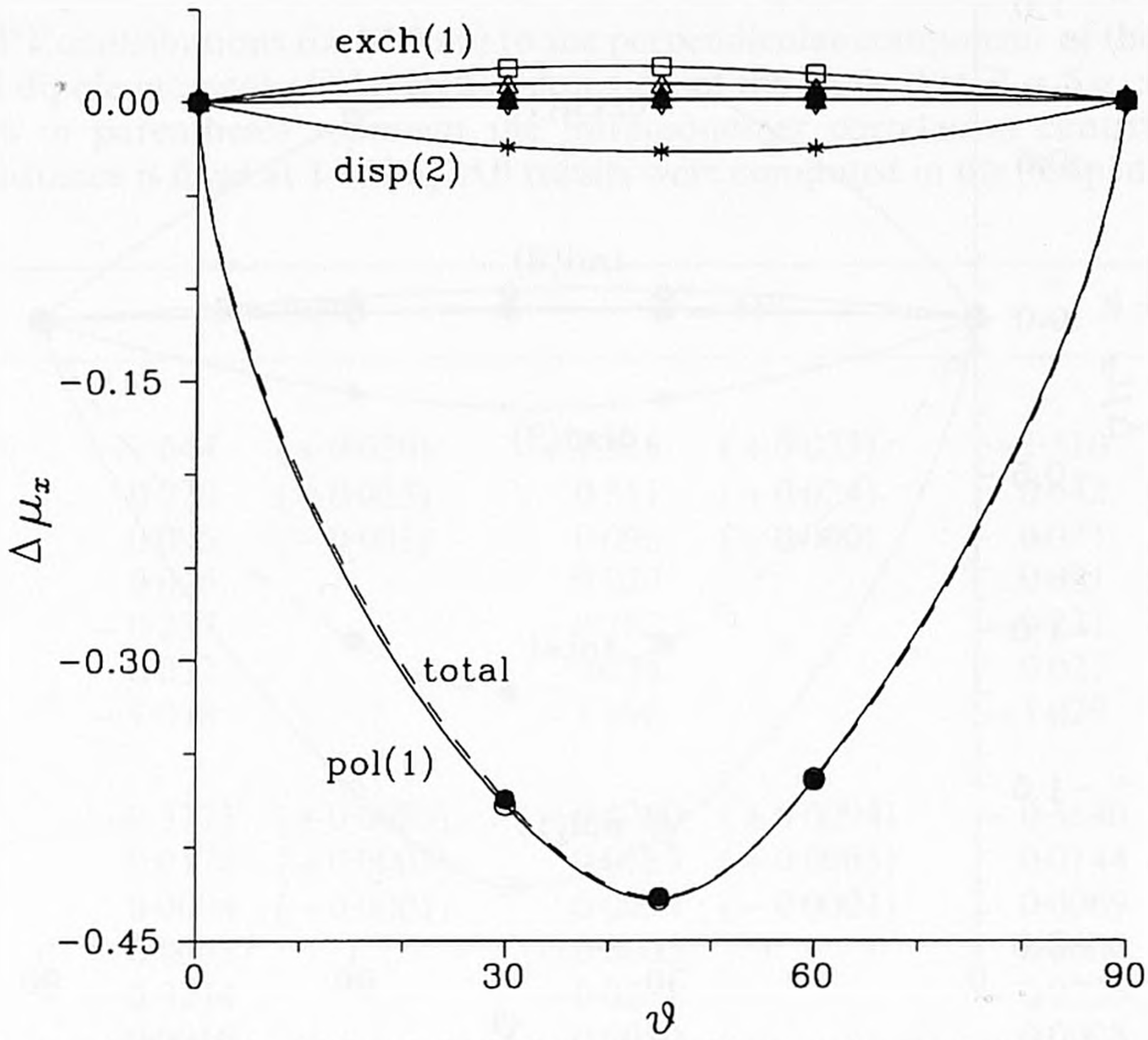

Figure 4. Comparison of the different SAPT contributions to the perpendicular component of the interaction-induced dipole moment of He–H_2 (in 10^{-3} au) as functions of the angle ϑ at $R = 7\ a_0$. The H—H distance is fixed at 1·449 a_0. Labels as for figure 1.

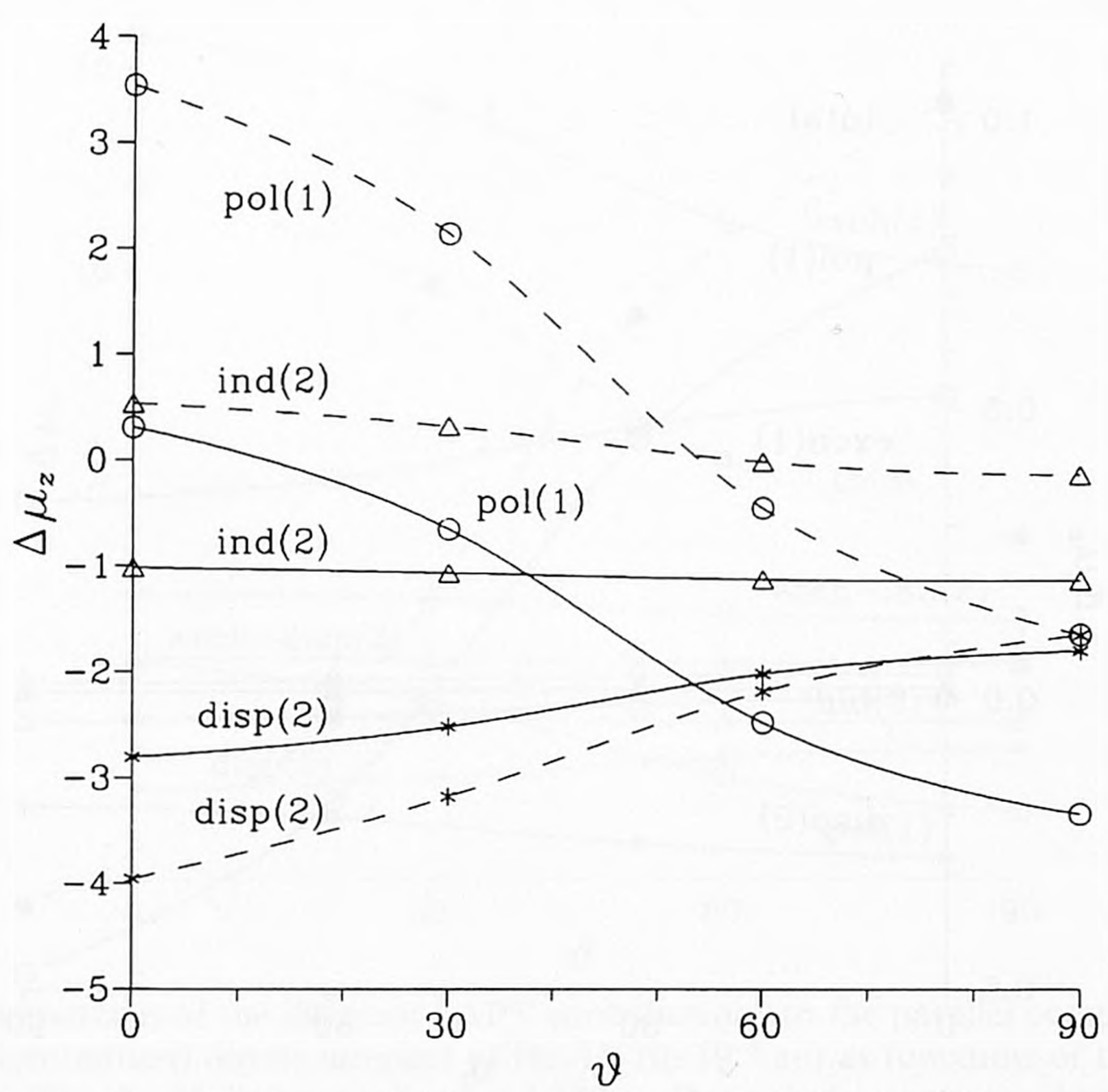

Figure 5. Comparison of the multipole-expanded (dashed lines) and non-expanded (solid lines) polarization contributions to the parallel component of the interaction-induced dipole moment of He–H_2 (in 10^{-3} au) as functions of the angle ϑ at $R = 5\ a_0$. The H—H distance is fixed at 1·449 a_0. The first-order contributions are labelled with open circles, the second-order induction contributions with open triangles, and the second-order dispersion contributions with crosses.

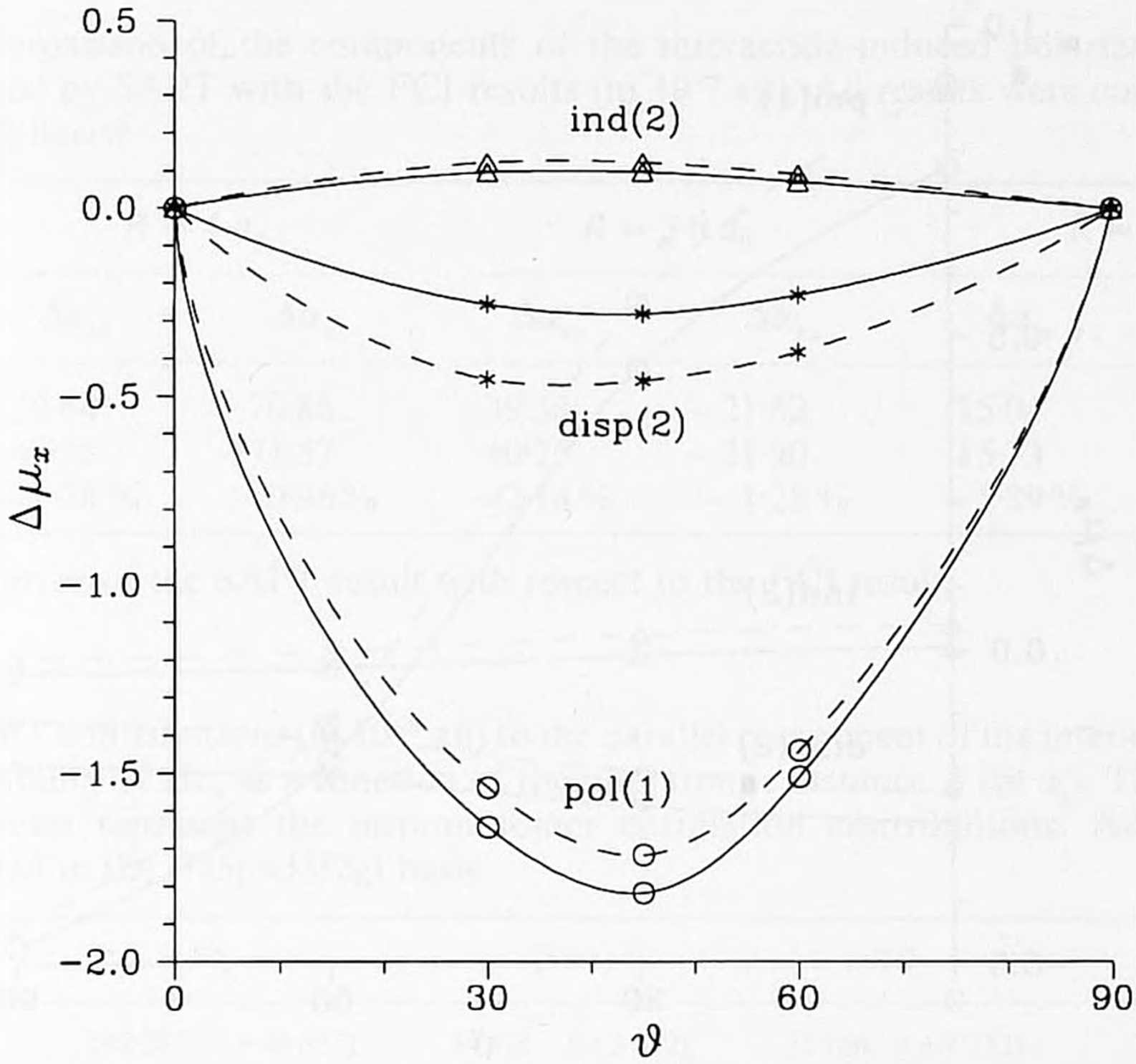

Figure 6. Comparison of the multipole-expanded (dashed lines) and non-expanded (solid lines) polarization contributions to the perpendicular component of the interaction-induced dipole moment of $He–H_2$ (in 10^{-3} au) as functions of the angle ϑ at $R = 5\ a_0$. The H—H distance is fixed at $1{\cdot}449\ a_0$. Labels as for figure 5.

included. We see that charge overlap gives a negative contribution to the parallel component of the dipole, which explains that at $\vartheta = 90°$ the ratio between the $R = 5\ a_0$ to $R = 7\ a_0$ values of $\Delta\mu^{(1)}_{z,\mathrm{pol}}(= 7{\cdot}06)$ is much larger than the value $(7/5)^4$ $(= 3{\cdot}84)$, which one would expect expression (40). We also observe that at $5\ a_0$ and $\vartheta = 0$ the negative contribution from charge penetration quenches to a large extent the positive long-range contribution to $\Delta\mu^{(1)}_{z,\mathrm{pol}}$.

Since the multipole-expanded expressions for the interaction-induced dipole moments are sometimes used in the calculations of the collision-induced spectra (see, e.g., [100]), it is interesting to check in somewhat more detail whether this approximation reproduces the polarization contributions to $\Delta\mu_i$ correctly. In figures 5 and 6 we compare the anisotropy of $\Delta\mu^{(1)}_{i,\mathrm{pol}}$, $\Delta\mu^{(2)}_{i,\mathrm{ind}}$, and $\Delta\mu^{(2)}_{i,\mathrm{disp}}$, $i = z$ or x, as computed by SAPT and from the multipole expansion at the intermolecular distance of $5\,a_0$. The region around $5\,a_0$ dominates the infrared absorption, (see, e.g., [10]). In figures 7 and 8 we compared $\Delta\mu^{(1)}_{i,\mathrm{pol}}$, $\Delta\mu^{(2)}_{i,\mathrm{ind}}$, and $\Delta\mu^{(2)}_{i,\mathrm{disp}}$, $i = z$ or x, computed by SAPT and in the multipole approximation at $R = 7\ a_0$. Since the multipole-expanded calculations were performed at the same level of theory and in the same basis sets, all differences can be attributed to the neglect of the charge overlap (damping) effects. An inspection of figure 5 shows that the multipole approximations to the electrostatic, induction, and dispersion contributions reproduce the shape of the anisotropy of these components. The actual values are rather different, however, for instance, the electrostatic and dispersion contributions are strongly overestimated, while the induction term is underestimated. It is interesting to note that the multipole approximations to $\Delta\mu^{(1)}_{z,\mathrm{pol}}$ and $\Delta\mu^{(2)}_{z,\mathrm{ind}}$ do not even reproduce correctly the signs of these components. This suggests that the electrostatic and induction terms are dominated by the exponential

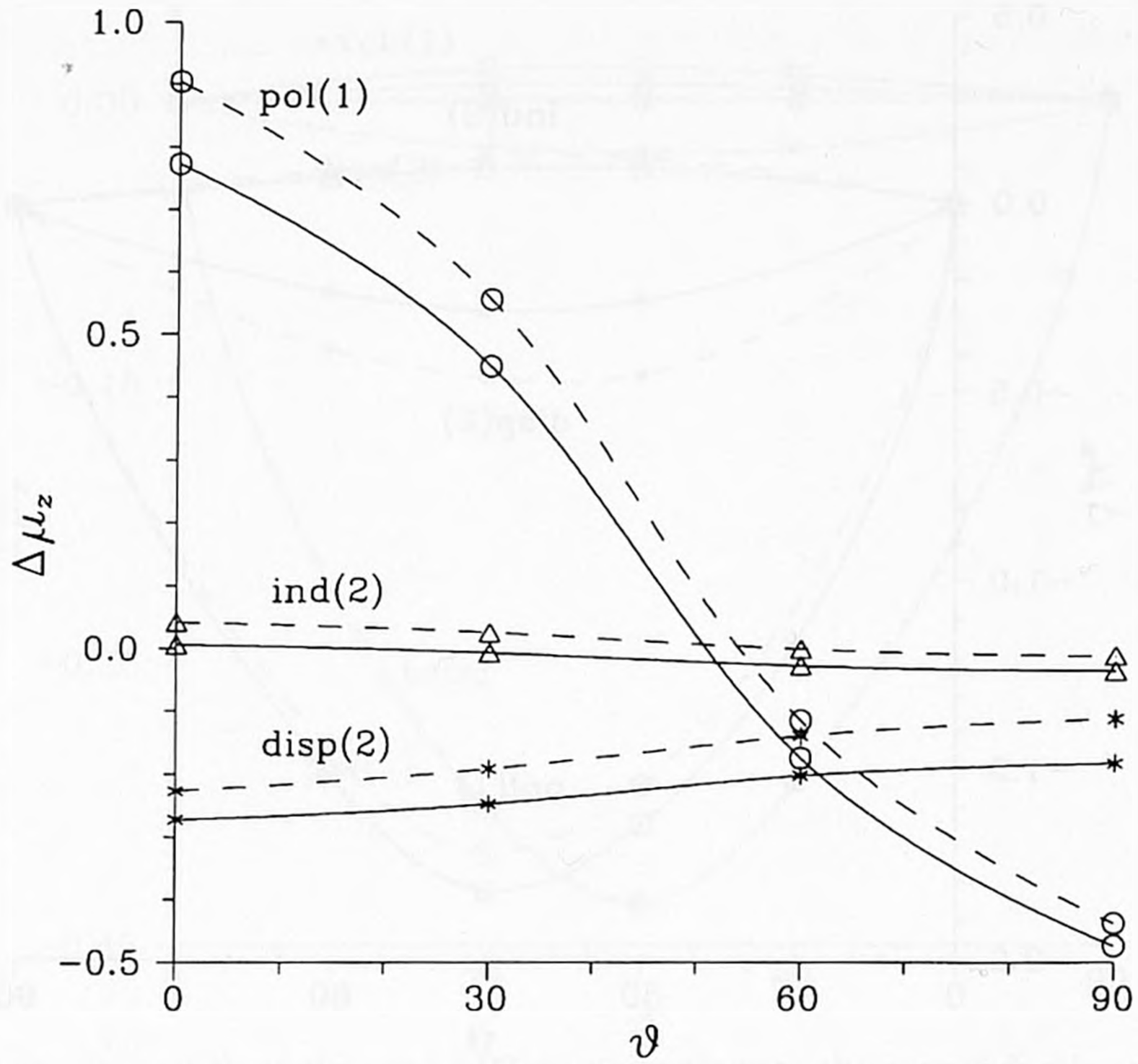

Figure 7. Comparison of the multipole-expanded (dashed lines) and non-expanded (solid lines) polarization contributions to the parallel component of the interaction-induced dipole moment of He–H_2 (in 10^{-3} au) as functions of the angle ϑ at $R = 7\ a_0$. The H—H distance is fixed at $1{\cdot}449\ a_0$. Labels as for figure 5.

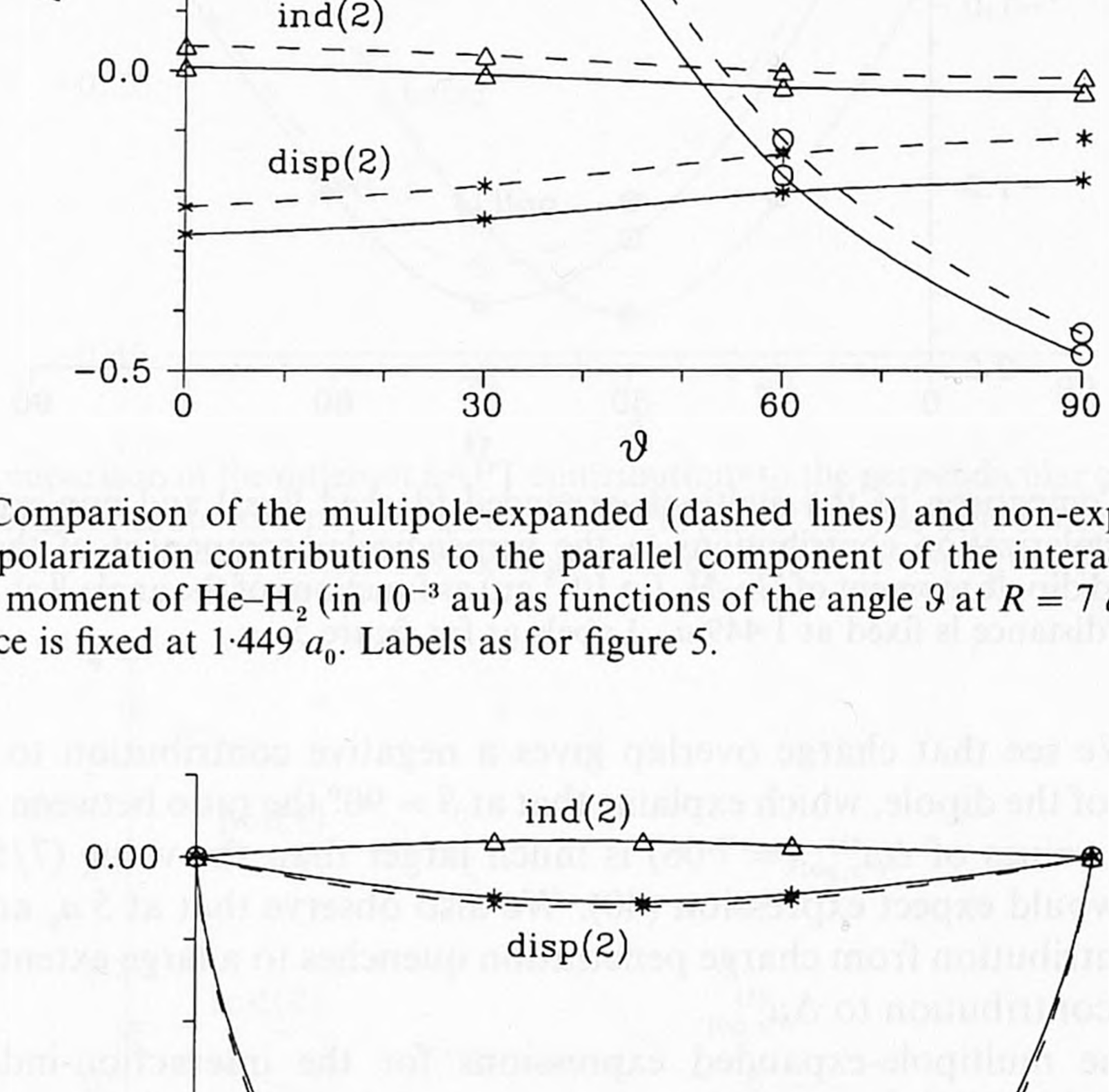

Figure 8. Comparison of the multipole-expanded (dashed lines) and non-expanded (solid lines) polarization contributions to the perpendicular components of the interaction-induced dipole moment of He–H_2 (in 10^{-3} au) as functions of the angle ϑ at $R = 7\ a_0$. The H—H distance is fixed at $1{\cdot}449\ a_0$. Labels as for figure 5.

Table 4. Comparison of the components of the interaction-induced polarizability of He_2 computed by SAPT with the FCI results (in 10^{-3} au). All results were computed in the [5s3p2d] basis.

	$R = 4\ a_0$		$R = 5{\cdot}6\ a_0$		$R = 8\ a_0$	
	$\Delta\alpha_{zz}$	$\Delta\alpha_{xx}$	$\Delta\alpha_{zz}$	$\Delta\alpha_{xx}$	$\Delta\alpha_{zz}$	$\Delta\alpha_{xx}$
SAPT	39·64	−70·88	39·38	−21·62	15·04	−7·32
FCI	40·35	−71·57	40·25	−21·90	15·33	−7·41
Δ[a]	−1·74 %	−0·96 %	−2·14 %	−1·28 %	−1·89 %	−1·21 %

[a] Relative error of the SAPT result with respect to the FCI result.

Table 5. SAPT contributions (in 10^{-3} au) to the parallel component of the interaction-induced polarizability of He_2 as a function of the interatomic distance R (in a_0). The numbers in parentheses represent the intramonomer correlation contributions. All results were computed in the [7s5p4d3f2g] basis.

R	3·0		5·6		7·0		10·0	
$\Delta\alpha^{(1)}_{zz,\mathrm{pol}}$	342·217	(+28·037)	44·626	(+3·542)	22·184	(+1·732)	7·572	(+0·587)
$\Delta\alpha^{(1)}_{zz,\mathrm{exch}}$	−616·256	(−66·056)	−9·498	(−1·315)	−0·627	(−0·097)	−0·001	(−0·000)
$\Delta\alpha^{(2)}_{zz,\mathrm{ind}}$	143·300	(+8·840)	1·507	(+0·093)	0·217	(+0·013)	0·020	(+0·001)
$\Delta\alpha^{(2)}_{zz,\mathrm{exch\text{-}ind}}$	−129·820		−0·799		−0·034		−0·000	
$\Delta\alpha^{(2)}_{zz,\mathrm{disp}}$	57·033		2·976		0·603		0·045	
$\Delta\alpha^{(2)}_{zz,\mathrm{exch\text{-}disp}}$	−7·158		−0·250		−0·021		0·000	
$\Delta\alpha_{zz}$	−5·744		39·645		22·370		7·653	

charge-overlap contributions. Consequently, these contributions cannot be represented by introducing damping functions into the multipole-expanded expressions. The situation is somewhat different for the perpendicular component $\Delta\mu_x$ (figure 6). The ϑ dependence of $\Delta\mu^{(1)}_{x,\mathrm{pol}}$, $\Delta\mu^{(2)}_{x,\mathrm{ind}}$, and $\Delta\mu^{(2)}_{x,\mathrm{disp}}$ is again predicted correctly by the multipole approximation. Also, the actual values of the electrostatic and induction contributions are rather well reproduced (within $\sim 10\,\%$ or better), while the dispersion term is again overestimated.

5.2. *Interaction-induced polarizability of He_2*

In table 4 we compare the components of the interaction-induced polarizability computed at the FCI level with the SAPT results in the same basis set. For all distances considered in this table, the SAPT results underestimate the values from the FCI calculations by 2 % at worst. Similarly as in the case of He–H_2 the convergence rate of the SAPT expansion shows a weak dependence on the interatomic distance.

In tables 5 and 6 we analyse the computed values of $\Delta\alpha_{zz}$ and $\Delta\alpha_{xx}$ in terms of SAPT contributions at various interatomic distances. The largest contributions to the components of the interaction-induced polarizability are given by the first-order terms. Except for the smallest interatomic distance ($R = 3\ a_0$), the sum $\Delta\alpha^{(1)}_{ii,\mathrm{pol}} + \Delta\alpha^{(1)}_{ii,\mathrm{exch}}$, $i = z$ or x, reproduces more than 88 % of the total interaction induced polarizability. Observe further than the intra-atomic correlation contributions to $\Delta\alpha^{(1)}_{ii,\mathrm{pol}}$ and $\Delta\alpha^{(1)}_{ii,\mathrm{exch}}$ are important. For the electrostatic term this contribution

Table 6. SAPT contributions (in 10^{-3} au) to the perpendicular component of the interaction-induced polarizability of He_2 as a function of the interatomic distance R (in a_0). The numbers in parentheses represent the intramonomer correlation contributions. All results were computed in the [7s5p4d3f2g] basis.

R	3·0		5·6		7·0		10·0	
$\Delta\alpha^{(1)}_{xx,\mathrm{pol}}$	−114·194	(−7·854)	−21·407	(−1·651)	−11·037	(−0·857)	−3·785	(−0·293)
$\Delta\alpha^{(1)}_{xx,\mathrm{exch}}$	−112·193	(−13·393)	−1·140	(−0·198)	−0·057	(−0·011)	−0·000	(−0·000)
$\Delta\alpha^{(2)}_{xx,\mathrm{ind}}$	10·974	(+0·854)	0·203	(+0·012)	0·047	(+0·003)	0·005	(+0·000)
$\Delta\alpha^{(2)}_{xx,\mathrm{exch-ind}}$	1·300		0·000		0·000		0·000	
$\Delta\alpha^{(2)}_{xx,\mathrm{disp}}$	18·550		0·923		0·217		0·021	
$\Delta\alpha^{(2)}_{xx,\mathrm{exch-disp}}$	−2·888		−0·047		−0·003		0·000	
$\Delta\alpha_{xx}$	−185·932		−21·442		−10·851		−3·752	

Table 7. Multipole contributions (in 10^{-3} au) to the parallel component of the interaction-induced polarizability of He_2 as a function of the interatomic distance R (in a_0). All results were computed in the [7s5p4d3f2g] basis. The numbers in parentheses represent the relative error of the multipole result with respect to the SAPT result (cf. table 5).

R	3·0		5·6		7·0		10·0	
$\Delta\alpha^{(1)}_{zz,\mathrm{pol}}$	280·315	(−18·1 %)	43·097	(−3·4 %)	22·066	(−0·5 %)	7·569	(−0·0 %)
$\Delta\alpha^{(2)}_{zz,\mathrm{ind}}$	47·498	(−66·9 %)	0·717	(−52·0 %)	0·178	(−18·0 %)	0·020	(−0·0 %)
$\Delta\alpha^{(2)}_{zz,\mathrm{disp}}$	217·150	(280·4 %)	1·984	(−33·3 %)	0·426	(−29·0 %)	0·041	(−9·0 %)

Table 8. Multipole contributions (in 10^{-3} au) to the perpendicular component of the interaction-induced polarizability of He_2 as function of the interatomic distance R (in a_0). All results were computed in the [7s5p4d3f2g] basis. The numbers in parentheses represent the relative error of the multipole result with respect to the SAPT result (cf. table 6).

R	3·0		5·6		7·0		10·0	
$\Delta\alpha^{(1)}_{xx,\mathrm{pol}}$	−140·157	(22·7 %)	−21·548	(0·7 %)	−11·033	(−0·0 %)	−3·784	(−0·0 %)
$\Delta\alpha^{(2)}_{xx,\mathrm{ind}}$	14·051	(28·0 %)	0·188	(−7·4 %)	0·046	(−2·0 %)	0·005	(−0·0 %)
$\Delta\alpha^{(2)}_{xx,\mathrm{disp}}$	99·999	(439·1 %)	0·860	(−6·8 %)	0·196	(−10·0 %)	0·021	(−0·0 %)

represents 7–8 % of the uncorrelated result, while for the exchange component it amounts to as much as 10–20 %. The interatomic correlation contributions are of relatively modest importance, being of the same order of magnitude as the intra-atomic correlation contributions. For example, in the region of the potential minimum ($R = 5{\cdot}6\ a_0$) the sum of the dispersion and exchange–dispersion terms contributes to $\Delta\alpha_{zz}$ and $\Delta\alpha_{xx}$ only 7 % and 4 %, respectively.

Finally, in tables 7 and 8 we compare the multipole-expanded and non-expanded polarization contributions to the parallel and perpendicular components of the interaction-induced polarizability of He_2. For both components the multipole expansion yields results which differ considerable from the non-expanded data. Except for large interatomic distances, the multipole expansion is seen clearly to diverge. It is interesting to note that the rate of divergence is different for the perpendicular and parallel components, as well as for various contributions. For instance, at intermediate distances near the van der Waals minimum the electrostatic contribution is rather well represented by the multipole approximation, while the induction and dispersion terms

are underestimated, especially for the parallel component. Hence, we conclude that the full inclusion of the charge-overlap effects is very important. The difference between the expanded and non-expanded dispersion contribution to the parallel component at $R = 10\ a_0$ may be caused partly by numerical errors in the finite field method.

6. Conclusion

A symmetry-adapted perturbation theory has been formulated for the calculation of the interaction-induced electrical properties of weakly bound complexes, and general asymptotic expressions have been derived for the first- and second-order contributions to the collision-induced dipole moments and polarizabilities in terms of the multipole moments and (hyper)polarizabilities of the isolated monomers. Numerical results for model four-electron systems (He–H_2 and He_2) reported in the present paper suggest that the SAPT method could be used routinely in the calculation of the collision-induced properties. The major features of the SAPT approach may be summarized as follows.

(1) The interaction-induced properties are computed directly as a sum of well defined physical contributions, which have a clear, partly classical, partly quantum, physical interpretation.
(2) Since the interaction-induced properties are obtained directly (not as a difference of large numbers), they are free from basis set superposition errors.
(3) The multipole expansion is not employed, so all charge penetration (damping) effects are included automatically.
(4) The multipole expansion has its use, however, in offering asymptotic constraints to the fits of the SAPT contributions to the interaction-induced dipole moments and polarizabilities. This is because the long-range contribution can be computed separately in terms of monomer properties (multipole moments and (hyper)polarizabilities), which in turn can be calculated in the same basis and at the same level of approximation as used in the SAPT approach.
(5) The convergence of the SAPT expansion for the interaction-induced dipole moment and polarizability appears to be satisfactory, at least for model four-electron systems like He–H_2 and He_2.

Of course, the final judgement of the accuracy of the computed collision-induced dipole moments and polarizabilities is by comparison with experiment. In [23 and 101] we report the collision-induced Raman spectra and second dielectric virial coefficients for the He diatom computed using the interaction-induced polarizability tensor from SAPT calculations. A similar study of the collision-induced infrared spectrum of He–H_2 is in progress in our group.

We thank dr. Piotr Piecuch for his help with Zarrabian's FCI program. This work was supported by the Netherlands Foundation of Chemical Research (SON), the Netherlands Organization for Scientific Research (NWO), and Polish Scientific Research Council (KBN), grant No. 3 T09A 072 09.

Appendix A

12*j* and 15*j*-symbols

For the convenience of the reader, we give the 12*j* symbol of the first kind occurring in equation (35), expressed as a single sum of products of four 6*j* symbols [91],

$$\begin{Bmatrix} l_A & l_B & L_B & \lambda \\ l_A+l_B & l'_B & L_A & 1 \\ L & l'_A+l'_B & l'_A & \lambda_A \end{Bmatrix} = \sum_x [x](-1)^{L_A+L_B+L+\lambda+\lambda_A+1+x}$$

$$\times \begin{Bmatrix} l_A & L & x \\ l'_A+l'_B & l_B & l_A+l_B \end{Bmatrix} \begin{Bmatrix} l_B & l'_A+l'_B & x \\ l'_A & L_B & l'_B \end{Bmatrix} \begin{Bmatrix} L_B & l'_A & x \\ \lambda_A & \lambda & L_A \end{Bmatrix} \begin{Bmatrix} \lambda & \lambda_A & x \\ l_A & L & 1 \end{Bmatrix}. \quad \text{(A 1)}$$

A similar expression holds for the 12*j* symbol of the first kind in equation (48). Note that in this paper only integer quantum numbers appear. We simplified the phases accordingly.

Analogously, the 15*j* symbol of the third kind appearing in equation (47) can be written as a single sum of products of one 6*j* and two 9*j* symbols [91],

$$\begin{Bmatrix} L_A & l'_A & L_B & l'_B & \lambda & l'_A+l'_B \\ \lambda_A & & \lambda_B & & L & \\ 1 & l_A & 1 & l_B & l & l_A+l_B \end{Bmatrix} = \sum_x [x](-1)^{\lambda_B+l'_B+1+x}$$

$$\times \begin{Bmatrix} L_B & 1 & x \\ l_B & l'_B & \lambda_B \end{Bmatrix} \begin{Bmatrix} L_B & 1 & x \\ L_A & 1 & \lambda_A \\ \lambda & l & L \end{Bmatrix} \begin{Bmatrix} l'_B & l_B & x \\ l'_A & l_A & \lambda_A \\ l'_A+l'_B & l_A+l_B & L \end{Bmatrix}. \quad \text{(A 2)}$$

The other 15*j* symbol of the third kind appearing in this paper (equation (49)) can be expressed similarly.

Appendix B

Special formulas for He_2

Below we list the multipolar dispersion contributions to the collision induced polarizabilities of two identical S state atoms. We write

$$(\Delta\alpha_0^{(11)0})^{(2)}_{\text{disp}}(R) \approx -\sqrt{3}\left(\frac{A_6}{R^6}+\frac{A_8}{R^8}+\frac{A_{10}}{R^{10}}\right) \quad \text{(B 1)}$$

and

$$(\Delta\alpha_0^{(11)2})^{(2)}_{\text{disp}}(R) \approx \frac{2}{\sqrt{6}}\left(\frac{B_6}{R^6}+\frac{B_8}{R^8}+\frac{B_{10}}{R^{10}}\right), \quad \text{(B 2)}$$

cf. equations (57) and (55). The coefficients A_n and B_n are

$$A_6 = -\frac{2}{3\pi}\sqrt{3}\int_0^\infty \alpha_0^{(11)0}(i\omega)\,\gamma_0^{(((11)01)11)0}(i\omega,0,0)\,\mathrm{d}\omega$$

$$A_8 = \frac{1}{\pi}\sqrt{5}\int_0^\infty \alpha_0^{(11)0}(i\omega)\,\gamma_0^{(((22)01)11)0}(i\omega,0,0)\,\mathrm{d}\omega$$

$$+\frac{1}{\pi}\sqrt{5}\int_0^\infty \alpha_0^{(22)0}(i\omega)\,\gamma_0^{(((11)01)11)0}(i\omega,0,0)\,\mathrm{d}\omega$$

$$-\frac{2}{\pi}\int_0^\infty \beta_0^{((21)11)0}(i\omega,0)\,\beta_0^{((21)11)0}(i\omega,0)\,\mathrm{d}\omega$$

$$A_{10} = -\frac{4}{3\pi}\sqrt{7}\int_0^\infty \alpha_0^{(33)0}(i\omega)\,\gamma_0^{(((11)01)11)0}(i\omega,0,0)\,\mathrm{d}\omega$$

$$-\frac{14}{3\pi}\sqrt{3}\int_0^\infty \alpha_0^{(22)0}(i\omega)\,\gamma_0^{(((22)01)11)0}(i\omega,0,0)\,\mathrm{d}\omega$$

$$-\frac{4}{3\pi}\sqrt{7}\int_0^\infty \alpha_0^{(11)0}(i\omega)\,\gamma_0^{(((33)01)11)0}(i\omega,0,0)\,\mathrm{d}\omega$$

$$+\frac{8}{3\pi}\sqrt{14}\int_0^\infty \beta_0^{((32)11)0}(i\omega,0)\,\beta_0^{((21)11)0}(i\omega,0)\,\mathrm{d}\omega$$

$$B_6 = -\frac{1}{5\pi}\sqrt{15}\int_0^\infty \alpha_0^{(11)0}(i\omega)\,\gamma_0^{(((11)21)11)0}(i\omega,0,0)\,\mathrm{d}\omega$$

$$B_8 = \frac{6}{5\pi}\int_0^\infty \alpha_0^{(22)0}(i\omega)\,\gamma_0^{(((11)21)11)0}(i\omega,0,0)\,\mathrm{d}\omega$$

$$+\frac{12}{35\pi}\sqrt{35}\int_0^\infty \alpha_0^{(11)0}(i\omega)\,\gamma_0^{(((22)21)11)0}(i\omega,0,0)\,\mathrm{d}\omega$$

$$+\frac{12}{35\pi}\sqrt{210}\int_0^\infty \alpha_0^{(11)0}(i\omega)\,\gamma_0^{(((31)21)11)0}(i\omega,0,0)\,\mathrm{d}\omega$$

$$-\frac{48}{5\pi}\int_0^\infty \beta_0^{((21)11)0}(i\omega,0)\,\beta_0^{((21)11)0}(i\omega,0)\,\mathrm{d}\omega$$

$$B_{10} = -\frac{2}{7\pi}\sqrt{35}\int_0^\infty \alpha_0^{(33)0}(i\omega)\,\gamma_0^{(((11)21)11)0}(i\omega,0,0)\,\mathrm{d}\omega$$

$$-\frac{10}{7\pi}\sqrt{21}\int_0^\infty \alpha_0^{(22)0}(i\omega)\,\gamma_0^{(((22)21)11)0}(i\omega,0,0)\,\mathrm{d}\omega$$

$$-\frac{30}{7\pi}\sqrt{14}\int_0^\infty \alpha_0^{(22)0}(i\omega)\,\gamma_0^{(((31)21)11)0}(i\omega,0,0)\,\mathrm{d}\omega$$

$$-\frac{5}{21\pi}\sqrt{210}\int_0^\infty \alpha_0^{(11)0}(i\omega)\,\gamma_0^{(((33)21)11)0}(i\omega,0,0)\,\mathrm{d}\omega$$

$$-\frac{10}{7\pi}\sqrt{35}\int_0^\infty \alpha_0^{(11)0}(i\omega)\,\gamma_0^{(((42)21)11)0}(i\omega,0,0)\,\mathrm{d}\omega$$

$$+\frac{80}{7\pi}\sqrt{14}\int_0^\infty \beta_0^{((32)11)0}(i\omega,0)\,\beta_0^{((21)11)0}(i\omega,0)\,\mathrm{d}\omega$$

References

[1] Birnbaum, G. (editor), 1985, *Phenomena Induced by Intermolecular Interactions*, NATO ASI Series B, Vol. 127 (New York: Plenum Press).

[2] Tabisz, G. C., and Neuman, M. N. (editors), 1995, *Collision- and Interaction-Induced Spectroscopy*, NATO ASI Series C, Vol. 452 (Dordrecht: Kluwer).

[3] Crawford, M. E., Welsh, H. L., MacDonald, J. C. F., and Locke, J. L., 1950, *Phys. Rev.*, **80**, 469.

[4] CHISHOLM, D. A., and WELSH, H. L., 1954, *Can J. Phys.*, **32**, 291.
[5] FROMMHOLD, L., 1994, *Collision-Induced Absorption in Gases* (Cambridge University Press).
[6] LEVINE, H. B., and BIRNBAUM, G. 1968, *Phys. Rev. Lett.*, **20**, 439.
[7] MCTAGUE, J. P., and BIRNBAUM, G., 1968, *Phys. Rev. Lett.*, **21**, 661.
[8] MCTAGUE, J. P., and BIRNBAUM, G. 1971, *Phys. Rev.* A, **3**, 1376.
[9] FROMMHOLD, L., 1981, *Adv. chem. Phys.*, **46**, 1.
[10] WORMER, P. E. S., and VAN DIJK, G., 1979. *J. chem. Phys.*, **70**, 5696.
[11] SADLEJ, J., 1979, *Spectrochim. Acta* A, **35**, 681.
[12] MEYER, W., and FROMMHOLD, L., 1994, *Theoret. Chim. Acta*, **88**, 201.
[13] MEYER, W., and FROMMHOLD, L., 1986, *Phys. Rev.* A, **33**, 3807.
[14] MEYER, W., and FROMMHOLD, L., 1986, *Phys. Rev.* A, **34**, 2771.
[15] FROMMHOLD, L., and MEYER, W., 1987, *Phys. Rev.* A, **35**, 632; 1990, *Phys. Rev.* A, **41**, 534.
[16] MEYER, W., and FROMMHOLD, L., 1986, *Phys. Rev.* A, **34**, 2936.
[17] MEYER, W., FROMMHOLD, L., and BIRNBAUM, G. 1989, *Phys. Rev.* A, **39**, 2434.
[18] MEYER, W., BORYSOW, A., and FROMMHOLD, L., 1989, *Phys. Rev.* A, **40**, 6931.
[19] FOWLER, P. W., and SADLEJ, A. J., 1992, *Molec. Phys.*, **77**, 709.
[20] BERNS, R. M., WORMER, P. E. S., MULDER, F., and VAN DER AVOIRD, A., 1978, *J. chem. Phys.*, **69**, 2102.
[21] DACRE, P. D., 1978, *Molec. Phys.*, **36**, 541.
[22] DACRE, P. D., 1982, *Molec. Phys.*, **45**, 17.
[23] MOSZYNSKI, R., HEIJMEN, T. G. A., WORMER, P. E. S., and VAN DER AVOIRD, A., 1996, *J. chem. Phys.*, **104**, 6997.
[24] DACRE, P. D., 1981, *Can J. Phys.*, **59**, 1439.
[25] WOLINSKI, K., and SADLEJ, A. J., 1992, *Molec. Phys.*, **75**, 221.
[26] HUNT, K. L. C., and LI, X., 1995, *Collision- and Interaction-Induced Spectroscopy*, edited by G. C. Tabisz and M. N. Neuman NATO ASI Series C, Vol. 452. (Dordrecht: Kluwer), p. 61.
[27] MEYER,, W., and FROMMHOLD, L., 1995, *Collision- and Interaction-Induced Spectroscopy*, edited by G. C. Tabisz and M. N. Neuman NATO ASI Series C, vol. 452. (Dordrecht: Kluwer), p. 441.
[28] MEYER, W., BORYSOW, A., and FROMMHOLD, L., 1993, *Phys. Rev.* A, **47**, 4065.
[29] DACRE, P. D., and FROMMHOLD, L., 1982, *J. chem. Phys.*, **76**, 3447.
[30] HUNT, K. L. C., 1980, *Chem. Phys. Lett.*, **70**, 336.
[31] GALATRY, L., and GHARBI, T., 1980, *Chem. Phys. Lett.*, **75**, 427.
[32] HUNT, K. L. C., 1984, *J. chem. Phys.*, **80**, 393.
[33] HUNT, K. L. C., and BOHR, J. E., 1985, *J. chem. Phys.*, **83**, 5198.
[34] BOHR, J. E., and HUNT, K. L. C., 1987, *J. chem. Phys.*, **86**, 5441.
[35] BOHR, J. E., and HUNT, K. L. C., 1987, *J. chem. Phys.*, **87**, 3821.
[36] LI, X., and HUNT, K. L. C., 1994, *J. chem. Phys.*, **100**, 9276.
[37] BUCKINGHAM, A. D., MARTIN, P. H., and WATTS, R. S., 1973, *Chem. Phys. Lett.*, **21**, 186.
[38] BUCKINGHAM, A. D., and CLARKE, K. L., 1978, *Chem. Phys. Lett.*, **57**, 321.
[39] CLARKE, K. L., MADDEN, P. A., and BUCKINGHAM, A. D., 1978, *Molec. Phys.*, **36**, 301.
[40] HUNT, K. L. C., ZILLES, B. A., and BOHR, J. E., 1981, *J. chem. Phys.*, **75**, 3079.
[41] HUNT, K. L. C., and BOHR, J. E., 1986., *J. chem. Phys.*, **84**, 6141.
[42] LI, X., and HUNT, K. L. C., 1994, *J. chem. Phys.*, **100**, 7875.
[43] FOWLER, P. W., 1990, *Chem. Phys.*, **143**, 447.
[44] BISHOP, D. M., and PIPIN, J., 1993, *J. chem. Phys.*, **98**, 4003.
[45] BISHOP, D. M., and PIPIN, J., 1992, *J. chem. Phys.*, **97**, 3375; 1993, *J. chem. Phys.*, **99**, 4875.
[46] FOWLER, P. W., HUNT, K. L. C., KELLY, H. M., and SADLEJ, A. J., 1995, *J. chem. Phys.*, **100**, 2932.
[47] JASZUNSKI, M., JØRGENSEN, P., and RIZZO, A., 1995, *Theoret. Chim. Acta*, **90**, 291.
[48] BYERS BROWN, W., and WHISNANT, D. M., 1973, *Molec. Phys.*, **25**, 1385.
[49] LACEY, A. J., and BYERS BROWN, W., 1974, *Molec. Phys.*, **27**, 1013.
[50] OXTOBY, D. W., and GELBART, W. M., 1975, *Molec. Phys.*, **30**, 535.
[51] SADLEJ, J., 1979, *Adv. molec. Relax. Processes*, **16**, 14.
[52] HUNT, K. L. C., and BUCKINGHAM, A. D., 1980, *J. chem. Phys.*, **72**, 2832.

[53] HILTON, P. R., and OXTOBY, D. W., 1981, *J. chem. Phys.*, **74**, 1824.
[54] JUANOS I TIMONEDA, J., and HUNT, K. L. C., 1986, *J. chem. Phys.*, **84**, 3954.
[55] JASZUNSKI, M., 1987, *Chem. Phys. Lett.*, **135**, 565.
[56] SZALEWICZ, K., and JEZIORSKI, B., 1979, *Molec. Phys.*, **38**, 191.
[57] JEZIORSKI, B., MOSZYNSKI, R., RYBAK, S., and SZALEWICZ, K., 1989, *Many-Body Methods in Quantum Chemistry*, edited by U. Kaldor, Lecture Notes in Chemistry, Vol. 52 (New York: Springer-Verlag), p. 65.
[58] RYBAK, S., JEZIORSKI, B., and SZALEWICZ, K., 1991, *J. chem. Phys.*, **95**, 6576.
[59] MOSZYNSKI, R., JEZIORSKI, B., RATKIEWICZ, A., and RYBAK, S., 1993, *J. chem. Phys.*, **99**, 8856.
[60] MOSZYNSKI, R., JEZIORSKI, B., and SZALEWICZ, K., 1994, *J. chem. Phys.*, **100**, 1312.
[61] MOSZYNSKI, R., JEZIORSKI, B., RYBAK, S., SZALEWICZ, K., and WILLIAMS, H. L., 1994, *J. chem. Phys.*, **100**, 5080.
[62] MOSZYNSKI, R., CYBULSKI, S. M., and CHALASINSKI, G., 1994, *J. chem. Phys.*, **100**, 4998.
[63] WILLIAMS, H. L., SZALEWICZ, K., MOSZYNSKI, R., and JEZIORSKI, B., 1995, *J. chem. Phys.*, **103**, 4586.
[64] JEZIORSKI, B., and KOLOS, W., 1977, *Int. J. Quantum Chem.* Suppl. 1, **12**, 91.
[65] JEZIORSKI, B., and KOLOS, W., 1982, *Molecular Interactions*, Vol. 3, edited by H. Ratajczak and W. J. Orville-Thomas (New York: Wiley), p. 1.
[66] CWIOK, T., JEZIORSKI, B., KOLOS, W., MOSZYNSKI, R., and SZALEWICZ, K.,1992, *J. chem. Phys.*, **97**, 7555.
[67] CWIOK, T., JEZIORSKI, B., KOLOS, W., MOSZYNSKI, R., and SZALEWICZ, K., 1994, *J. molec. Struct. Theochem*, **307**, 135.
[68] WORMER, P. E. S., MULDER, F., and VAN DER AVOIRD, A., 1977, *Int. J. Quantum Chem.*, **11**, 959.
[69] VAN DER AVOIRD, A., WORMER, P. E. S., MULDER, F., and BERNS, R. M., 1980, *Topics Current Chem.*, **93**, 1 (1980); in the course of the present work we found a phase error in equation (24) of this reference: the factor $(-1)^{L_A+L_B+L}$ was inadvertently omitted.
[70] ORR, B. J., and WARD, J. F., 1971, *Molec. Phys.*, **20**, 513.
[71] WORMER, P. E. S., and HETTEMA, H., 1992, *J. chem. Phys.*, **97**, 5592.
[72] WORMER, P. E. S., and HETTEMA, H., 1992, Polcor package, Nijmegen.
[73] MOSZYNSKI, R., JEZIORSKI, B., DIERCKSEN, G. H. F., and VIEHLAND, L. A., 1994, *J. chem. Phys.*, **101**, 4697.
[74] MOSZYNSKI, R., WORMER, P. E. S., and VIEHLAND, L. A., 1994, *J. Phys.* B, **27**, 4933.
[75] WILLIAMS, H. L., SZALEWICZ, K., JEZIORSKI, B., MOSZYNSKI, R., and RYBAK, S., 1993, *J. chem. Phys.*, **98**, 1279.
[76] MOSZYNSKI, R., WORMER, P. E. S., JEZIORSKI, B., and VAN DER AVOIRD, A., 1994, *J. chem. Phys.*, **101**, 2811.
[77] MOSZYNSKI, R., WORMER, P. E. S., and VAN DER AVOIRD, A., 1995, *J. chem. Phys.*, **102**, 8385.
[78] MOSZYNSKI, R., KORONA, T., WORMER, P. E. S., and VAN DER AVOIRD, A., 1995, *J. chem. Phys.*, **103**, 321.
[79] LOTRICH, V. F., WILLIAMS, H. L., SZALEWICZ, K., JEZIORSKI, B., MOSZYNSKI, R., WORMER, P. E. S., and VAN DER AVOIRD, A., 1995, *J. chem. Phys.*, **103**, 6076.
[80] JEZIORSKI, B., MOSZYNSKI, R., and SZALEWICZ, K., 1994, *Chem. Rev.*, **94**, 1887.
[81] MOSZYNSKI, R., JEZIORSKI, B., WORMER, P. E. S., and VAN DER AVOIRD, A., 1994, *Chem. Phys. Lett.*, **221**, 161.
[82] MOSZYNSKI, R., JEZIORSKI, B., VAN DER AVOIRD, A., and WORMER, P. E. S., 1994, *J. chem. Phys.*, **101**, 2825.
[83] VAN DER AVOIRD, A., WORMER, P. E. S., and MOSZYNSKI, R., 1994, *Chem. Rev.*, **94**, 1931.
[84] JEZIORSKA, M., JEZIORSKI, B., and CIZEK, J., 1987, *Int. J. Quantum Chem.*, **32**, 149.
[85] MOSZYNSKI, R., HEIJMEN, T. G. A., and JEZIORSKI, B., 1996, *Molec. Phys.*, **88**, 741.
[86] SADLEJ, A. J., 1980, *Molec. Phys.*, **39**, 1249.
[87] JASZUNSKI, M., 1980, *Molec. Phys.*, **39**, 777.
[88] JEZIORSKI, B., BULSKI, M., and PIELA, L., 1975, *Int. J. Quantum Chem.*, **10**, 281.
[89] CHALASINSKI, G., and JEZIORSKI, B., 1977, *Theoret. Chim. Acta*, **46**, 277.
[90] BRINK, D. M., and SATCHLER, G. R., 1975, *Angular Momentum* (Oxford: Clarendon Press).

[91] YUTSIS, A. P., LEVINSON, I. B., and VANAGAS, V. V., 1962, *Mathematical Apparatus of the Theory of Angular Momentum* (Jerusalem: Israel Program for Scientific Translations).
[92] VAN DUIJNEVELDT, F. B., 1971, IBM Research Report RJ945; the exponents and contraction coefficients of the s functions for the He atom are available from the present authors on request.
[93] GUTOWSKI, M., VERBEEK, J., VAN LENTHE, J. H., and CHALASINSKI, G., 1987, *Chem. Phys.*, **111**, 396.
[94] HOBZA, P., SCHNEIDER, B., SAUER, J., CARSKY, P., and ZAHRADNIK, R. 1987, *Chem. Phys. Lett.*, **134**, 418.
[95] JEZIORSKI, B., MOSZYNSKI, R., RATKIEWICZ, A., RYBAK, S., SZALEWICZ, K., and WILLIAMS, H. L., 1993, *Methods and Techniques in Computational Chemistry*, Vol. B *Medium Size Systems*, edited by E. Clementi (Cagliari: STEF), p. 79.
[96] ZARRABIAN, S., SARMA, C. R., and PALDUS, J., 1989, *Chem. Phys. Lett.*, **155**, 183; HARRISON, R. J., and ZARRABIAN, S., 1989, *Chem. Phys. Lett.*, **158**, 393.
[97] BOYS, S. F., and BERNARDI, F., 1970, *Molec. Phys.*, **19**, 553.
[98] RIJKS, W., and WORMER, P. E. S., 1988, *J. chem. Phys.*, **88**, 5704.
[99] MEYER, W., HARIHARAN, P. C., and KUTZELNIGG, W., 1980, *J. chem. Phys.*, **72**, 1880.
[100] BORYSOW, A., and MORALDI, M., 1993, *J. chem. Phys.*, **99**, 8424.
[101] MOSZYNSKI, R., HEIJMEN, T. G. A., and VAN DER AVOIRD, A., 1995, *Chem. Phys. Lett*, **247**, 440.